

Dear Editor,

All comments and suggestions have been considered. Point by point responses to these comments are listed below. The marked-up manuscript version is attached below.

Referee report #1

General comments

I recommend that this manuscript should be published in ACP after the few (minor) technical corrections listed below have been addressed.

Specific comments

1. Previous review, specific comment 2 - Were the IOP1 and IOP2 samples analysed on the same day, or was the detector variation of the UHRMS monitored during the analysis period? The UHRMS will vary in sensitivity. Running samples days or weeks apart may result in a variation in the amount of species observed due to fluctuations in the UHRMS sensitivity (e.g. as the mass spectrometer becomes 'dirty', the detector sensitivity will decrease, affecting the ion intensity and subsequently the amount of species observed). This is particularly important in Figures 2 and 4 where the molecular formulae and ion abundances, respectively, are compared. If the samples were not analysed at the same time or if the detector sensitivity was not monitored, the authors would not be able to compare the ion abundance of the tracer compounds as shown in Figure 4. This is also likely to affect the comparison of the molecular formulae in Figure 2. The work presented here would then be only qualitative (rather than semi-quantitative). Were any attempts made to account for variations in detector sensitivity?

Author response - The instrument was routinely calibrated before the analysis. It must be noted that in the current study we used a nanoESI source where each sample is processed using a separate ESI tip and nozzle, so there is no carryover between samples. All samples were analysed in a random order and within 48-hours after extraction (to minimise possible methylation; therefore, the observed differences could not be attributed to the instrument contamination).

Further review - The specific comment above was in regards to detector variation, not contamination or carryover, whilst both will also affect ion intensities. The authors have not fully addressed the question. It is still unclear if all the samples were analysed at the same time or if the detector variation was monitored. The authors note that the instrument is routinely calibrated, although I suspect (based on the method details) this only for mass accuracy and not for detector variation. The instrument should notify the user during mass calibration if the ion intensities of the calibrants are too low, highlighting sensitivity issues. However I do recommend in future, that the authors run samples at the same time when they plan to compare ion intensities (if not already done so) or use standards to monitor detection variation.

We disagree with this comment. The image current from oscillating ion packages in Orbitrap is recorded by the instrument over time and thus changes in sensitivity is not an issue in Orbitrap compared to many other MS detectors. Furthermore, when the instrument (i.e. ion optics) will get contaminated over time, it will adjust the injection time, so the absolute

amount of ions in the Orbitrap detector for a given scan will always be the same (so the AGC target, unless the instrument is hitting the max IT). We assume the reviewer is referring to instruments like ToF, where a multi channel plate or a similar detector may age over time. Having said that, the routine calibration and transmission checks were performed which also included monitoring ion signal intensity. Moreover, blank samples were run after every 5 real samples, which showed no loss in the ion signal intensity. Considering that we run the analysis of our samples in three different mass ranges, in at least three analytical and instrumental replicates it is not feasible to perform the complete analysis of a large number of samples at 'the same time' (we assume the reviewer meant on the same day?).

The following statement has been added to the text: '*The calibration (as described in Kourtchev et al., 2013) and an ion transmission checks that include monitoring of ion signal intensity were routinely performed.*'

Technical corrections

1. Line 225 (previous review specific comment 23), why are some compounds fragile? Please expand or reference. Author response - The sentence has been extended to '...(e.g. highly oxygenated compounds)'. I don't agree that all highly oxygenated compounds are fragile. Please change to '(e.g. thermally labile)'.

corrected

2. Line 127, change the fraction '1/2' to the word 'half'.

corrected

3. Line 209, Change '10 000 particles' to '104 particles'

corrected

4. Line 261 and elsewhere; radical on OH not used throughout text. Please change all 'OH' to '°OH'

Word 'radical' has been added to OH throughout the text

5. Line 283, could methyl-nitrophenol C₇H₇NO₃ and methyl-nitrocatechol C₇H₇NO₄ also come from vehicular emissions (i.e. toluene oxidation products), given that the site is also affected by urban air pollution?

The vehicular source of methyl-nitrophenol C₇H₇NO₃ and methyl-nitrocatechol C₇H₇NO₄ has been added to the text: '*....as well as diesel exhaust.*'

Reviewer #2

Molecular composition of organic aerosols in central Amazonia: an ultra-high resolution mass spectrometry study

The following technical corrections are suggested. It would also be best that the final manuscript is proofread by a native English speaker because there are still some problems

with punctuation, such as, for example, the correct use of the comma (not listed in this report).

The manuscript has been initially proofread by several native speakers (who are coauthors of this paper).

Line 52: that of the wet period.

corrected

Line 53: from the forest

corrected

Line 62:, Andreae et al., 2015).

corrected

Line 77:, nitrooxy-organosulfates

Do not see the difference with the initial statement

Line 83: (Nozière et al., 2015).

corrected

Line 89: have a mass resolution

corrected

Line 92:, Nozière et al., 2015).

corrected

Line 157: LC-MS: make sure that “LC-MS” is used consistently throughout the text; sometimes use is made of “LC/MS”.

corrected

Line 231:however, a rather insignificant

corrected

Line 236: during daytime and

corrected

Line 240: consistent with recent studies,

corrected

Line 266: during the wet

Line 270: from the OH-initiated oxidation

corrected

Line 272: from the ozonolysis reaction

corrected

Line 273: of ion signal intensities (Note: ions are abundant; ion signals are intense; a field campaign could be intensive)

corrected (the word 'signal' is often omitted in this context in mass spectrometry literature as it is trivial in this field).

Line 293 and 295:ion signal intensities

corrected

Line 297: in the gas phase

corrected

Line 302: that the benzene

We disagree with this suggestion

Line 314:, the number of forest

corrected

Lines 316, 320, and 323: ion signal intensities

corrected

Line 321: showed a very good

corrected

Line 324: with the latter one

corrected

Lines 328, 333, and 334: ion signal intensity

corrected

Line 342: employed an alternative GC/MS

corrected

Line 349:, the highest CO

corrected

Line 361: have a DBE value above

corrected

Line 396: with a pyrene core

corrected

Line 407: from biomass burning sources.

corrected

Line 411: corresponding to other biomass burning OA markers, i.e., isomeric dimethyl-nitrocatechols

corrected

Line 413: of nitro-aromatic compounds

corrected

Line 418: a significantly larger

corrected

Line 419: but a smaller number

corrected

Line 430: to result in a different

corrected

Line 440: towards a more oxidized state ...

corrected

Line 447:, the effect was much lower compared to that

corrected

Line 448: A higher number

corrected

Line 468: in laboratory smog

Disagree, we are discussing the *specific* laboratory experiments published by Riva and co-authors.

Line 470: in the presence of acidified

corrected

Line 475: are a useful

corrected

Line 479: most abundant ion at

corrected

Line 489: be associated with

corrected

Line 491: that in most of the

corrected

Line 576: in Rondônia, Brazil:

corrected

Molecular composition of organic aerosols in central Amazonia: an ultra-high resolution mass spectrometry study

I. Kourtchev^{1,2*}, R.H.M. Godoi³², S. Connors¹, J.G. Levine⁴³, A. Archibald^{1,54}, A.F.L. Godoi³², S.L. Parolovo³², C.G.G. Barbosa³², R.A.F. Souza⁶⁵, A.O. Manzi⁷⁶, R. Seco⁸⁷, S. Sjostedt⁹⁸, J.-H. Park¹⁰⁹, A. Guenther^{87,110}, S. Kim⁸⁷, J. Smith^{124,132}, S.T. Martin^{143,154} and M. Kalberer^{1*}

¹Department of Chemistry, University of Cambridge, Cambridge, CB2 1EW, UK

²[Department of Chemistry and Environmental Research Institute, University College Cork, Cork, Ireland](#)

³²Environmental Engineering Department, Federal University of Parana, Curitiba, Brazil

⁴³School of Geography Earth & Environmental Sciences, University of Birmingham, Birmingham, B15 2TT, UK

⁵⁴NCAS climate, University of Cambridge, Cambridge, CB2 1EW, UK

⁶⁵State University of Amazonas, Av. Darcy Vargas, 1200, 69065-020, Manaus-AM, Brazil

⁷⁶Instituto Nacional de Pesquisas da Amazônia (INPA), Clima e Ambiente (CLIAMB), Manaus-AM, Brazil

⁸⁷Department of Earth System Science, University of California, Irvine CA 92697, USA

⁹⁸NOAA ESRL Chemical Sciences Division, Boulder CO, USA.

¹⁰⁹National Institute of Environmental Research, Republic of Korea

¹¹⁰Pacific Northwest National Laboratory, Richland WA, USA

¹²⁴Atmospheric Chemistry Division, National Center for Atmospheric Research, Boulder CO, USA

¹³²Dept of Chemistry, University of California, Irvine CA, USA

¹⁴³Sch. Eng. & Appl. Sci., Harvard University, Cambridge, MA 02138 USA

¹⁵⁴Dep. Earth & Planetary Sciences, Harvard University, Cambridge, MA 02138 USA

*Corresponding authors: I. Kourtchev (i.kourtchev@ucc.ieink22@cam.ac.uk) and M. Kalberer (mk594@cam.ac.uk)

Abstract

The Amazon basin plays key role in atmospheric chemistry, biodiversity and climate change. In this study we applied nanoelectrospray (nanoESI) ultrahigh resolution mass spectrometry (UHR-MS) for the analysis of the organic fraction of PM_{2.5} aerosol samples collected during dry and wet seasons at a site in central Amazonia receiving background air masses, biomass burning and urban pollution. Comprehensive mass spectral data evaluation methods (e.g., Kendrick Mass Defect, Van Krevelen diagrams, carbon oxidation state and aromaticity equivalent) were used to identify compound classes and mass distributions of the detected species. Nitrogen and/or sulfur containing organic species contributed up to 60% of the total identified number of formulae. A large number of molecular formulae in organic aerosol (OA) were attributed to later-generation nitrogen- and sulfur-containing oxidation products, suggesting that OA composition is affected by biomass burning and other, potentially anthropogenic, sources. Isoprene derived organo sulfate (IEPOX-OS) was found as the most dominant ion in most of the analysed samples and strongly followed the concentration trends of the gas-phase anthropogenic tracers confirming its mixed anthropogenic-biogenic origin. The presence of oxidised aromatic and nitro-aromatic compounds in the samples suggested a strong influence from biomass burning especially during the dry period. Aerosol samples from the dry period and under enhanced biomass burning conditions contained a large number of molecules with high carbon oxidation state and an increased number of aromatic compounds compared to that from the wet period. The results of this work demonstrate that the studied site is influenced not only by biogenic emissions from the forest but also by biomass burning and potentially other anthropogenic emissions from the neighboring urban environments.

Keywords: organic aerosol, ultra-high resolution mass spectrometry, molecular composition, IEPOX-OS, Amazon.

Introduction

The Amazon basin plays key role in atmospheric chemistry, biodiversity and climate change (Keller et al., 2009; Andreae et al., 2015). The Amazon rainforest is an important source of Biogenic Volatile Organic Compound (BVOC) emissions to the atmosphere (Greenberg et al., 2004; Alves et al., 2015), which give rise to secondary organic aerosol (SOA) through reaction with atmospheric oxidants (i.e. O_3 , $OH\cdot$ and $NO_3\cdot$) (e.g., Martin et al., 2010). SOA particles scatter and absorb solar and terrestrial radiation, influence cloud formation, participate in chemical reactions in the atmosphere, and thus are suggested to play an important role in climate change (Andreae and Crutzen, 1997; Haywood and Boucher, 2000; Hallquist et al., 2009; Pöschl et al., 2010). Aerosol optical properties, which govern the ability to absorb solar radiation, strongly depend on SOA composition (Laskin et al., 2015). It has been shown that organic nitrates, nitrooxy-organosulfates and organic sulfates may contribute to light absorption by SOA (e.g., Song et al., 2013; Jacobson, 1999; Lu et al., 2011; Laskin et al., 2015). Chemical interactions between anthropogenic and biogenic aerosol precursors can play a significant role in the formation of SOA (Goldstein et al., 2009; Hoyle et al., 2011; Kleinman et al., 2015). For example, anthropogenic nitrogen oxides (NO_x) and sulfur dioxide (SO_2) are shown to react with a range of BVOCs leading to formation of organic nitrates (e.g., Roberts, 1990; Day et al., 2010; Fry et al., 2014), nitroxy-organosulfates and organosulfates (Surratt et al., 2008; Budisulistiorini et al., 2015). Much remains to be explored in terms of the molecular diversity of these compounds in the atmosphere.

A comprehensive knowledge of aerosol molecular composition, which in turn leads to better understanding of aerosol sources, is required for the development of effective air pollution mitigation strategies. However, identification of the organic aerosol composition, remains a major analytical challenge (Nozière et al., 2015). Organic aerosol is composed of thousands of organic compounds, which cover a wide range of physical and chemical properties (Goldstein and Galbally, 2007) making it difficult to find a single analytical technique for a detailed chemical analysis at the molecular level. Methods based on ultrahigh resolution mass

spectrometry (UHRMS) have shown great potential in solving this longstanding problem. UHR mass spectrometers (e.g., Fourier transform ion cyclotron resonance MS and Orbitrap MS) have mass resolution power that is at least one order of magnitude higher ($\geq 100\,000$) than conventional MS and high mass accuracy (< 5 ppm) and thus, when coupled with soft ionisation techniques (e.g., electrospray ionisation (ESI)), can provide a detailed molecular composition of the organic aerosol (Nizkorodov et al., 2011, ~~Nozière~~Nozière et al., 2015). Direct infusion ESI-UHRMS has been applied successfully for the analysis of aerosol samples from remote (e.g., boreal forest in Finland, Pico Island of the Azores archipelago), rural (e.g., Millbrook, USA; Harcum, USA; K-Puszt, Hungary) and urban (e.g., Cambridge, UK, Birmingham, UK, Cork, Ireland, Shanghai, China and Los Angeles, USA) locations (Wozniak et al., 2008; Schmitt-Kopplin et al., 2010; Kourtchev et al., 2013; 2014; Tao et al., 2014; Dzepina et al., 2015). UHRMS has proven to be extremely useful in assessing chemical properties of the SOA.

The aim of this study was to investigate the detailed molecular composition of organic aerosol from a site that received air masses from a wide range of origins, including the background atmosphere of Amazonia, biomass burning and urban pollution plumes. The measurements were performed as a part of the *Observations and Modeling of the Green Ocean Amazon* (GoAmazon2014/5) campaign (Martin et al., 2016). The location of the research site where aerosol was collected for this study is ~69 km downwind of Manaus (population 2 million), intersected background and polluted air with day-to-day variability in the position of the Manaus plume. The study designed served as a laboratory for investigating anthropogenic perturbations to biogenic processes and atmospheric chemistry.

Methods

Sampling site

Aerosol sampling was conducted at site “T3” of GoAmazon2014/5 located at -3.2133° and -60.5987° . $35^{\circ}55'32''$ W. The T3 site is located in the pasture area, ~2.5 km from the rainforest.

The air masses arriving to the sampling site often passed over the single large city (Manaus) in the region. Detailed descriptions of the site and instrumentation are provided in Martin et al. (2015).

PM_{2.5} aerosol samples were collected on 47 mm polycarbonate filters Nuclepore, using a Harvard impactor (Air Diagnostics, Harrison, ME, EUA) with flow rate of 10 L min⁻¹ from 5 to 26 March 2014 and 5 Sept to 04 Oct of 2014, which were during Intensity Operating Periods 1 and 2 (IOP1 and IOP2) of GoAmazon2014/5, respectively, corresponding to the traditional periods of wet and dry seasons of Amazonia. The sampling durations are shown in the Table SI1. The airflow through the sampler was approximately 10 L min⁻¹. After collection, the aerosol samples were transferred into Petri dishes and stored in the freezer at -4°C until analysis.

Aerosol Sample Analysis

Fifteen samples, 5 from IOP2 and 10 from IOP1, were extracted and analysed using a procedure described elsewhere (Kourtchev et al., 2014; Kourtchev et al., 2015). Depending on the aerosol loading of the analysed samples, a part (~~1/2~~half to whole) of the filter was extracted in methanol (Optima TM LC/MS grade, Fisher Scientific) in a chilled ice slurry, filtered through a Teflon filter (0.2 µm, ISODiscTM Supelco) and reduced by volume using a nitrogen line to achieve approximately 0.3 µg of aerosol per µL methanol. Several samples with the highest aerosol loading were divided into two parts for both direct infusion and LC/MS analyses while the samples with the lowest loading were only analysed using direct infusion analysis. The LC/MS portion was further evaporated to 20 µL and diluted to 100 µL by aqueous solution of formic acid (0.1%). The final extracts were analysed as described in Kourtchev et al. (2013) using a high-resolution LTQ Orbitrap Velos mass spectrometer (Thermo Fisher, Bremen, Germany) equipped with ESI and a TriVersa Nanomate robotic nanoflow chip-based ESI (Advion Biosciences, Ithaca NY, USA) sources. The Orbitrap MS was calibrated using an Ultramark 1621 solution (Sigma-Aldrich, UK). The mass accuracy of the instrument was below

1 ppm. The instrument mass resolution was 100 000 at m/z 400. The ion transmission settings were optimised using a mixture of camphor sulfonic acid (20 ng μL^{-1}) glutaric acid (30 ng μL^{-1}), and *cis*-pinonic acid (30 ng μL^{-1}) in methanol and Ultramark 1621 solution.

Direct infusion UHRMS analysis

The ionisation voltage and back pressure of the nanoESI direct infusion source were set at - 1.4 kV and 0.8 psi, respectively. The inlet temperature was 200 °C and the sample flow rate was approximately 200–300 nL min⁻¹. The negative ionisation mass spectra were collected in three replicates at two mass ranges (m/z 100–650 and m/z 150–900) and processed using Xcalibur 3.1 software (Thermo Fischer Scientific Inc.). Similar to our preceding studies (Kourtchev et al., 2015) the average percentage of common peaks between analytical replicates was ~80%. This is also in agreement with literature reports for similar data analysis (Sleighter et al., 2012). The identification of IEPOX organosulfates was performed by comparing MS fragmentation patterns and chromatographic elution time with a synthesised IEPOX-OS standard which was provided by Dr Surratt from University of North Carolina. It must be noted that due to competitive ionisation of analytes in the direct infusion ESI analysis of the samples with a very complex matrix (i.e., aerosol extracts), the ion intensities do not directly reflect the concentration of the molecules in the sample (Oss et al., 2010); therefore, data shown in this work is semi-quantitative.

LC/MS analysis

LC/MS ESI parameters were as follows: spray voltage -3.6 kV; capillary temperature 300 °C; sheath gas flow 10 arbitrary units, auxiliary gas flow 10; sweep gas flow rate 5; S-lens RF level 58 %. LC/(-)ESI-MS analysis was performed using an Accela system (Thermo Scientific, San Jose, USA) coupled with LTQ Orbitrap Velos MS and a T3 Atlantis C18 column (3 μm ; 2.1 x 150 mm; Waters, Milford, USA). The sample extracts were injected at a flow rate of 200 μL min⁻¹. The mobile phases consisted of 0.1% formic acid (v/v) (A) and methanol (B). The applied gradient was as follows: 0–3 min 3% B, 3–25 min from 3 to 50% B (linear), 25–43 min from

50 to 90% B (linear), 43–48 min from 90 to 3% B (linear), and kept for 12 min at 3% B. The Collision Induced Dissociation (CID) settings for MS/MS analysis are reported in Kourtchev et al (2015).

High resolution MS data analysis

The direct infusion data analysis was performed using procedures described in detail by Kourtchev et al. (2013). The calibration (as described in Kourtchev et al., 2013), ion transmission checks that include monitoring of ion signal intensity were routinely performed. Briefly, for each sample analysis, 60–90 mass spectral scans were averaged into one mass spectrum. Molecular formulae assignments were made using Xcalibur 3.1 software using the following constraints $^{12}\text{C} \leq 100$, $^{13}\text{C} \leq 1$, $^1\text{H} \leq 200$, $^{16}\text{O} \leq 50$, $^{14}\text{N} \leq 5$, $^{32}\text{S} \leq 2$, $^{34}\text{S} \leq 1$. The data processing was performed using a Mathematica 8.0 (Wolfram Research Inc., UK) code developed in-house that utilises a number of additional constraints described in previous studies (Kourtchev et al., 2013; Kourtchev et al., 2015). Only ions that appeared in all three replicates were kept for evaluation. The background spectra obtained from the procedural blanks were also processed using the rules mentioned above. The formulae lists of the background spectra were subtracted from those of the ambient (or chamber) sample and only formulae with a sample/blank peak intensity ratio ≥ 10 were retained

The Kendrick Mass Defect (KMD) is calculated from the difference between the nominal mass of the molecule and the exact KM (Kendrick, 1963). Kendrick mass of the CH_2 unit is calculated by renormalising the exact IUPAC mass of CH_2 (14.01565) to 14.00000.

Benzene and isoprene measurements

For benzene and isoprene analysis we used a high-resolution selective-reagent-ionisation proton transfer reaction time-of-flight mass spectrometer (SRI-PTR-TOF-MS 8000, Ionicon Analytik, Austria). A description of the PTR-TOF-MS instrument and the data reduction process used are provided elsewhere (Graus et al. 2010; Müller et al. 2013). Background of the instrument was measured regularly by passing ambient air through a platinum catalyst

heated to 380 °C. Sensitivity calibrations were performed by dynamic dilution of VOCs using several multi-component gas standards (Apel Riemer Environmental Inc., Scott-Marrin, and Air Liquide, USA). The calibration cylinders contained acetaldehyde, acetone, benzene, isoprene, α -pinene, toluene and trichlorobenzene, among others. During IOP1, the instrument was operated with H_3O^+ reagent ion and at a drift tube pressure of 2.3 mbar, voltage of 600 V, and temperature of 60 °C, corresponding to a a field density ratio E/N ratio of 130 Td (E being the electric field strength and N the gas number density; 1 Td = 10^{-17} V cm⁻²). During IOP2, the reagent ion was NO^+ and the drift tube settings were 2.3 mbar, 350 V, and 60 °C, resulting in an E/N ratio of 76 Td. The sampling was done with 1 min time resolution and the instrument detection limit for benzene and isoprene were below 0.02 and 0.04 ppbv, respectively.

Air mass history analysis

Air mass history analysis was done for the sampling period using the Numerical Atmospheric-dispersion Modeling Environment (NAME) model, developed by the UK Met Office (Maryon et al., 1991). NAME is a Lagrangian model in which particles are released into 3D wind fields from the operational output of the UK Met Office Unified Model meteorology data (Davies et al., 2005). These winds have a horizontal resolution of 17 km and 70 vertical levels up that reach ~80 km. In addition, a random walk technique was used to model the effects of turbulence on the trajectories (Ryall and Maryon, 1998). To allow the calculation of air mass history for the average sampling time (which varied between samples, 24, 36 or 48 hours), ~~10⁴-000~~ 10⁴ particles per hour were released continuously from the T3 site. The trajectories travelled back in time for 3 days with the position of the particles in the lowest 100 m of the model atmosphere recorded every 15 min. The particle mass below 100 m was integrated over the 72 h travel time. The air mass history ('footprints') for the periods of the analysed filters are shown in Figure SI1. The majority of the three-day air mass footprints originated from the east, although wind direction showed variability nearer to the sampling site on some occasions e.g., sample MP14-17 (Fig. SI1). Almost all air masses pass over Manaus and

therefore highlight this city as a potential source. Some air masses also pass over Manacapuru, but this is rare and the corresponding time-integrated concentrations are lower than the equivalent Manaus values.

Results and discussions

Figure 1 shows mass spectra from two typical samples collected during IOP1 and IOP2. The majority of the ions were associated with molecules below 500 Da although the measured mass goes up to 900 Da. Although ESI is a 'soft' ionisation technique resulting in minimal fragmentation, we cannot exclude the possibility that some of the detected ions correspond to fragments, also in light of the many relative fragile compounds (e.g., ~~thermally labile~~^{highly oxygenated} compounds) that constitute OA. The largest group of identified molecular formulae in all samples were attributed to molecules containing CHO atoms only (1051 ± 141 formulae during IOP2 and 820 ± 139 during IOP1), followed by CHON (537 ± 71 during IOP2 and 329 ± 71 during IOP1), CHOS (183 ± 34 during IOP2 and 137 ± 31 during IOP1) and CHONS (37 ± 11 during IOP2 and 28 ± 10 during IOP1) (Fig. 2). The number of molecular formulae containing CHO and CHON subgroups increased by ~20% from IOP1 to IOP2 period; however, ^a rather insignificant increase was observed for CHOS and CHONS subgroups. The Student's t-test showed that the observed difference for CHO ($p=0.0092$) and CHON ($p=0.00007$) subgroups between two seasons is statistically significant. This is consistent with the observed increase in odd reactive nitrogen species (NO_y) from IOP1 to IOP2 (Table SI1). Organic nitrates are believed to form in polluted air through reaction with nitrogen oxides during day^{time} and from reaction of NO_3^- with BVOCs during nighttime (Day et al., 2010; Ayres et al., 2015). The average concentration of NO_y during IOP1 was found to be on almost two times higher, which is possibly reflected in the increased number of organonitrates in the aerosol samples from IOP2. Moreover, the increase in the number of organonitrates during IOP2 is consistent with ~~the~~ recent studies, which demonstrated that organonitrates groups in aerosol particles may hydrolyse under high RH conditions (Liu et al., 2012). In this respect, while night time

maximum RH during both filter sampling periods was very similar (~90%), day-time RH during IOP1 was higher (89%) compared to that from the IOP2 period (66%) (Fig. SI2).

Carbon oxidation state (OS_C) introduced by Kroll et al. (2011) can be used to describe the composition of a complex mixture of organics undergoing oxidation processes. OS_C was calculated for each molecular formula identified in the mass spectra using the following equation:

$$OS_C = -\sum_i OS_i \frac{n_i}{n_C} \quad (\text{Eq. 1})$$

where OS_i is the oxidation state associated with element i , n_i/n_C is the molar ratio of element i to carbon within the molecule (Kroll et al., 2011).

Figure 3 shows overlaid OS_C plots for two samples from IOP1 and IOP2. Consistent with previous studies, the majority of molecules in the sampled organic aerosol had OS_C between -1.5 and $+1$ with up to 30 (n_C) carbon atoms throughout the selected mass range (m/z 100-650) (Kroll et al., 2011 and the references therein). The molecules with OS_C between -1 and $+1$ with 13 or less carbon atoms (n_C) are suggested to be associated with semivolatile and low-volatility oxidised organic aerosol (SV-OOA and LV-OOA) produced by multistep oxidation reactions. The molecules with OS_C between -0.5 and -1.5 with 7 or more carbon atoms are associated with primary biomass burning organic aerosol (BBOA) directly emitted into the atmosphere (Kroll et al., 2011). The cluster of molecules with OS_C between -1 and -1.5 and n_C less than 10 could be possibly associated with OH radical oxidation products of isoprene (Kourtchev et al., 2015), which is an abundant VOC in Amazon rain forest (Rasmussen and Khalil, 1988; Chen et al., 2015). The isoprene daytime average was above 1.5 ppbv during both seasons, with hourly campaign-averages reaching up to 2.3 and 3.4 ppbv for IOP1 and IOP2, respectively. In general, aerosol samples from IOP1 contained less oxidised molecules compared to those from IOP2. Wet deposition of aged or processed aerosol during the wet (i.e., IOP 2) sampling period cannot be the only reason for the observed differences in OS_C . It has been shown that different oxidation regimes to generate SOA (e.g., OH radical vs.

270 ozonolysis) can result in significantly different OSc of SOA (Kourtchev et al., 2015). For
 271 example, the SOA component from the OH radical initiated oxidation of α -pinene as well as
 272 BVOC mixtures had a molecular composition with higher OSc throughout the entire molecular
 273 mass range compared to that obtained from the ozonolysis reaction (Kourtchev et al., 2015).
 274 Figure 4 shows the distribution of ion signal intensities for selected tentatively identified tracer
 275 compounds for anthropogenic, biogenic and mixed sources in all 15 samples. The structural
 276 or isomeric information is not directly obtained from the direct infusion analysis; therefore, the
 277 identification of the tracer compounds was achieved by comparing MS/MS fragmentation
 278 patterns from authentic standards and published literature. The tracer compounds include
 279 anhydrosugars, structural isomers with a molecular formula $C_6H_{10}O_5$ at m/z 161.0456
 280 corresponding to levoglucosan, mannosan, galactosan and 1,6-anhydro- β -D-glucofuranose,
 281 which are regarded as marker compounds for biomass burning (Simoneit et al., 1999;
 282 Pashynska et al., 2002; Kourtchev et al., 2011). Nitrocatechols, with a molecular formula
 283 $C_6H_5NO_4$ (m/z 154.01458) are attributed to mixed anthropogenic sources, e.g., biomass and
 284 vehicular emissions and methyl-nitrocatechols ($C_7H_7NO_4$, m/z 168.03023) are important
 285 markers for biomass burning OA, formed from *m*-cresol emitted during biomass burning
 286 (Iinuma et al., 2010) as well as diesel exhaust. 3-methyl-1,2,3-butanetricarboxylic acid (3-
 287 MBTCA), with a molecular formula $C_8H_{12}O_6$ at m/z 203.05611, is an OH radical- initiated
 288 oxidation product of α - and β -pinene (Szmigielski et al., 2007), and regarded as a tracer for
 289 processed or biogenic SOA. Finally, isoprene epoxydiol organosulfate ester (IEPOX-OS), with
 290 a molecular formula $C_5H_{12}O_7S$ at m/z 215.0231, is shown in Figure 4. From studies in mid
 291 latitude environments it has been suggested that IEPOX-OS is formed through reactions
 292 between SO_x and isoprene oxidation products (Pye et al., 2013; Budisulistiorini et al., 2015)
 293 and thus can be used to observe the extent of SO_2 aging effects on the biogenic SOA. Direct
 294 infusion analysis suffers from competitive ionisation in the complex matrices and thus
 295 comparing ion intensities across samples has to be done with caution. Moreover, other
 296 compounds with similar molecular composition present in the aerosol matrix may also

contribute to the ion signal intensities of the discussed above compounds. All selected tracers showed very similar variations with benzene concentration that was measured in the gas-phase using PTR-MS (Fig. 3). Benzene, generally regarded as an anthropogenic species, has various sources including industrial solvent production, vehicular emissions and biomass burning (Hsieh et al., 1999; Seco et al., 2013; Friedli et al., 2001). Recent studies indicated that vegetation (leaves, flowers, and phytoplankton) emits a wide variety of benzenoid compounds to the atmosphere at substantial rates (Misztal et al., 2015). However, considering that benzene concentration correlated very well with another anthropogenic tracer CO ($R^2=0.77$, Figure SI3) during IOP1 and IOP2 periods, it is rather likely that the observed benzene concentrations were mainly due to anthropogenic emissions. During the sampling period, irrespectively of the season, air masses passed over the large city Manaus and small municipalities located near the T3 site (Figure SI1). It must be noted that due to rather low sampling resolution time (≥ 24 h) the molecular composition of all analysed samples is likely to be influenced by clean air masses and anthropogenic plumes from these urban locations which usually last only a few hours per day and thus individual urban plume events cannot be identified with the data analysed here. In Manaus natural gas is mainly used for heating and cooking and therefore, the contribution from these activities to biomass burning OA at our site is highly unlikely. During IOP1 much lower incidents of forest fires were observed compared to that during IOP2 (Martin et al., 2016). For example, the number of forest fires in the radius of 200 km from the sampling site varied between 0 to 340 fires (<http://www.dpi.inpe.br/proarco/bdqueimadas/>). This is reflected in the ion signal intensities of the particle phase biomass burning markers, i.e., anhydrosugars ($C_6H_{10}O_5$) and nitrocatechols ($C_6H_5NO_4$) and gas-phase benzene concentrations, which were significantly lower during IOP1 compared to that from IOP2, when on average more fires are observed.

It should be noted that ion signal intensities for anhydrosugars ($C_6H_{10}O_5$) and nitrocatechols ($C_6H_5NO_4$) showed a very good correlation ($R^2>0.7$) suggesting that nitrocatechols, observed at the sampling site, are mainly associated with biomass burning sources. The highest ion

signal intensities of these tracer compounds were observed during two periods: 7-9 September 2014 (sample MP14-128) and 27-28 September 2014 (sample MP14-148) with the latter one coinciding with highest incident of fires (340 fires). Although during 7-9 September (sample MP14-128) a significantly lower number (22 fires) of fires was observed compared to the period of 27-28 September 2014, lower wind speed occurring during 7-9 September suggests that high intensity of the biomass burning markers could be due to the biomass burning emissions from nearby sources. Between the T3 sampling site and Manaus (about 20 km east of the site), there are a number of small brick factories, which use wood to fire the kilns (Martin et al., 2016) and thus they are an additional local wood burning source besides the forest and pasture fires.

Interestingly the sample MP14-148 had the highest ion intensity corresponding to IEPOX-OS (Fig. 4), which also coincided with the strong increase of the ion intensity at m/z 96.95987 corresponding to $[\text{HSO}_4]^-$. This is consistent with organosulfates formation mechanism through reactive uptake of isoprene epoxydiols (IEPOX) in the presence of acidic sulfate seed (Surratt et al., 2010; Lin et al., 2012; 2013). A similar relationship between sulfate and organosulfates concentrations has been observed previously in field studies in the Southeastern US (Surratt et al., 2007, 2008, 2010; Lin et al., 2012, 2013). This is also in agreement with previous studies from Amazon where the highest levels of 2-methyltetrols were observed during the dry period which was characterised by biomass burning (and higher particle concentrations of sulfuric acid) (Claeys et al., 2010). Considering that Claeys et al (2010) employed an alternative GC/MS procedure with prior trimethylsilylation, 2-methyltetrol sulfates were converted to 2-methyltetrols and not detectable as separate OS compounds. It should be noted that the 27-28 September period (sample MP14-148) was marked by a very strong increase in the CO concentration (Fig. SI4). In mid-latitude environments it has been suggested that the production of anthropogenic SOA in an air mass, as it travels from an urban source region, can be estimated by using a relatively inert pollution tracer, such as CO occurring in the air mass (De Gouw et al., 2005; Hoyle et al., 2011). At T3 sampling site, the highest CO

concentrations are observed in air masses affected by biomass burning. Therefore, it is possible that organic aerosol in the sample MP14-148 has experienced the highest contribution from biomass burning as well as other anthropogenic activities.

To investigate the influence of anthropogenic activities (i.e., biomass burning) on a detailed molecular composition of organic aerosol at the T3 site we compared samples from the periods with the lowest (9 fires), moderately high (254 fires) and the highest (340 fires) incidents of fires occurring within 200 km around the site.

Figure 5 (a-c) shows H/C ratios of CHO containing formulae as a function of their molecular mass and double bond equivalent (DBE), which shows a degree of unsaturation of the molecule, for a sample with the lowest (a) moderately high (b) and highest incidents (c) of fires. One of the obvious differences between these samples is the abundance of ions with low H/C ratios (< 1). The majority of these ions have a DBE value above 7 indicating that they likely correspond to oxidised aromatic compounds, which are mainly of anthropogenic origin (Kourtchev et al., 2014; Tong et al., 2016). For example, the smallest polycyclic aromatic hydrocarbon (PAH), naphthalene with a molecular formulae $C_{10}H_8$ has an $H/C=0.8$ and $DBE=7$. The number of CHO containing formulae with high DBE equivalent and low H/C increased dramatically during the days with moderately high and high incidents of fires (Fig. 5a-c), suggesting that they are mainly associated with biomass burning. The largest grey circles in Fig 5(a-c) correspond to the ions at m/z 133.01425 (with neutral molecular formula $C_4H_6O_5$), m/z 187.0612 ($C_8H_{12}O_5$), m/z 201.07685 ($C_9H_{14}O_5$), m/z 203.05611 ($C_8H_{12}O_6$), and m/z 215.05611 ($C_9H_{12}O_6$) with $DBE < 6$.

Recent studies indicated that different families of compounds with heteroatoms (e.g. O, S) overlap in terms of DBE and thus may not accurately indicate the level of unsaturation of organic compounds. For example, the divalent atoms, such as oxygen and sulphur, do not influence the value of DBE, yet they may contribute to the potential double bonds of that molecule (Reemtsma 2009; Yassine et al., 2014). Yassine et al (2014) suggested using

aromaticity equivalent (X_c), to improve the identification and characterisation of aromatic and condensed aromatic compounds in WSOC. The aromaticity equivalent can be calculated as follows:

$$X_c = \frac{3(\text{DBE} - (mN_O + nN_S)) - 2}{\text{DBE} - (mN_O + nN_S)} \quad (\text{Eq. 2})$$

where 'm' and 'n' correspond to a fraction of oxygen and sulfur atoms involved in π -bond structures of a compound, which varies depending on the compound class. For example, carboxylic acids, esters, and nitro functional groups have $m=n=0.5$. For compounds containing functional groups such as aldehydes, ketones, nitroso, cyanate, alcohol, or ethers 'm' and 'n' are 1 or 0. Considering that ESI, in negative mode, is most sensitive to compounds containing carboxylic groups we, therefore, used $m=n=0.5$ for the calculation of the X_c . For molecular formulae with an odd number of oxygen or sulfur, the sum ($mN_O + nN_S$) in Eq. 2 was rounded down to the closest integer as detailed in Yassine et al (2014). The authors proposed that aromaticity equivalent with $X_c \geq 2.50$ and $X_c \geq 2.71$ as unambiguous minimum criteria for the presence of aromatics and condensed aromatics.

Expressing our data using aromaticity equivalents confirmed that the increase in the number of molecules with high DBE from the sample with the lowest to the highest incidents of fires was due to the increase in the number of aromatic and condensed aromatic compounds in the aerosol samples (Figures S15). Considering the Yassine et al. (2014) assignment criteria for the aromatic-reach matrices, the highest number of the aromatic compounds in the Amazon samples was observed for formulae with a benzene core structure ($X_c = 2.50$) followed by formulae with a pyrene core structure ($X_c = 2.83$), and an ovalene core structure ($X_c = 2.92$) as well as highly condensed aromatic structures or highly unsaturated compounds ($X_c > 2.93$). The largest grey circles in Figure S15a correspond to the ions at m/z 187.11357 with a neutral molecular formula $C_9H_{17}NO_3$ and m/z 281.26459 with a neutral molecular formula $C_{18}H_{35}NO$. The largest grey circles in Figure S15b and c correspond to the ions at m/z 154.0146, m/z

402 168.03023 and m/z 152.03532 with neutral molecular formulae $C_6H_5NO_4$, $C_7H_7NO_4$ and
403 $C_7H_7NO_3$, respectively.

404 Interestingly, a similar trend was observed for the molecules containing CHON subgroups
405 (Figure SI6). A number of CHON molecules with low H/C (<1) and high DBE (≥ 5) almost
406 doubled from the days with 9 to 340 fires (Figure SI7). Nitro-aromatic compounds, such as
407 nitrophenols (DBE=5) and N-heterocyclic compounds including 4-nitrocatechol and isomeric
408 methyl-nitrocatechols are often observed in the OA from ~~the~~ biomass burning sources
409 (Kitanovski et al., 2012a,b; Iinuma et al., 2010) and have been suggested as potential
410 contributors to light absorption by brown carbon (Laskin et al., 2015). It is worth mentioning
411 that aerosol samples affected by biomass burning contained another interesting ion at m/z
412 182.04588 with a neutral molecular formula $C_8H_9NO_4$, possibly corresponding to other
413 biomass burning OA markers, i.e., isomeric dimethyl-nitrocatechols (Kahnt et al., 2013). The
414 differences in the increased number of nitro-aromatic compounds in aerosol samples affected
415 by biomass burning are also apparent in overlaid Van Krevelen diagrams (Figure 6), which
416 show H/C and O/C ratios for each formula in a sample. Van Krevelen diagrams, can be used
417 to describe the overall composition or evolution of organic mixtures (Van Krevelen, 1993;
418 Nizkorodov et al., 2011; ~~Nozière~~ Nozière et al., 2015). Organic aerosol affected by biomass
419 burning contained a significantly larger number of CHON formulae with O/C < 0.5 and H/C <
420 1 (Fig. 6a and b, area B) but a smaller number of formulae with O/C < 0.5 and H/C > 1. (Fig.
421 6a and b, area A). While molecules with H/C ratios (<1.0) and O/C ratios (<0.5) (area A in Fig.
422 3) are generally associated with aliphatic compounds typically belong to oxidised aromatic
423 hydrocarbons, molecules with high H/C ratios (>1.5) and low O/C ratios (<0.5) (area B in Fig.
424 3) (Mazzoleni et al., 2010; 2012). Although the smaller number of nitro-aliphatic compounds
425 in the samples affected by biomass burning requires further investigation, it is possible that
426 they were oxidised in the polluted air by NO_x and O_3 (Zahardis et al., 2009; Malloy et al., 2009),
427 which production is significantly enhanced during fire events (e.g., Galanter et al., 2000). The
428 majority (up to 80%) of the CHON molecules in the analysed samples have O/C ratios < 0.7

(Fig. 6). The relatively low oxygen content suggests that these molecules include decreased nitrogen-containing compounds (Zhao et al, 2013). Although biomass burning material type is expected to result in a different molecular composition, the presence of a large number of molecules with low O/C ratio is consistent with the literature. For example, most of the CHON molecules in OA from wheat straw burning in K-puszt, Great Hungarian Plain in Hungary and biomass burning at Canadian rural sites (Saint Anicet, Quebec, and Canterbury, New Brunswick) had O/C ratios below 0.7 (Schmitt-Kopplin et al., 2010). In addition, the CHON molecules identified by LC/MS in biomass burning OA from Amazonia showed O/C ratios below 0.7, i.e., 4-nitrocatechol ($C_6H_5NO_4$; O/C = 0.67), isomeric methyl-nitrocatechols ($C_7H_7NO_4$; O/C = 0.57), and isomeric dimethyl-nitrocatechols ($C_8H_9NO_4$; O/C = 0.50) (Claeys et al., 2012).

Figure 7 shows overlaid OSc plots for OA from the days with low, moderately high and high incidents of fires. During the days affected by high and moderately high number of fires, OSc was shifted towards a more oxidised state for the CHO molecules containing more than 7 carbon atoms. The difference in OSc becomes even more pronounced with the increased number of carbons (e.g. >7 carbon atoms) in the detected molecular formulae. Interestingly, the affected ions with high OSc do not fall into the category of the BBOA (encircled area in Fig. 7) which are associated with primary particulate matter directly emitted into the atmosphere as defined in Kroll et al (2011).

At first glance, biomass burning seems to influence the number and intensity of the CHOS containing formulae; however, the effect was ~~at a much lower extent~~ compared to that for the CHO and CHON molecules (see discussion above). A-H higher number of CHOS containing molecules was observed in the sample (MP14-148) corresponding to the highest incident of fires (Figures 8a). Interestingly, IEPOX-OS was found to be very abundant in the sample that experienced the highest incidents of fires (Figure 8a). The significant IEPOX-OS mass was previously observed during a low-altitude flight campaigns at Northern California and southern Oregon at high NO conditions (> 500 pptv) (Liao et al., 2015). The authors explained this

observation by the transport or formation of IEPOX from isoprene hydroxynitrate oxidation (Jacobs et al., 2014) and higher sulphate aerosol concentrations occurring during their sampling period (Nguyen et al., 2014). This explanation is also consistent with our results. The ion at m/z 96.95987 corresponding $[\text{HSO}_4]^-$ in UHR mass spectra of the sample MP14-148 was three times more abundant compared that in the sample MP14-129 suggesting that particle acidity may be one of the reasons for the high abundance of the IEPOX-OS in this sample. Considering that the main sources of sulphate at T3 site are industrial pollution (e.g., power plants), natural and long range-sources, they could also be responsible for the high abundance of the sulphate and IEPOX-OS in the samples besides the overlapping biomass burning event. Noticeably, these samples not only contained a larger number of oxygenated CHOS-containing molecules with $\text{O/C} > 1.2$ but also molecules with $\text{O/C} < 0.6$ and H/C ranging from 0.4 to 2.2. Recent laboratory and field studies indicated the presence of a large number of aromatic and aliphatic OSs and sulfonates in OA and linked them to anthropogenic precursors (Tao et al., 2014; Wang et al., 2015; Riva et al., 2015; 2016; Kuang et al., 2016). Riva et al (2015, 2016) demonstrated formation of OSs and sulfonates in the laboratory smog chamber experiments from photooxidation of alkanes and PAHs, respectively. The authors indicated enhancement of organosulfates yields in the presence of ~~the~~-acidified ammonium sulphate seed and suggested that these OSs are mainly formed through reactive uptake of gas-phase epoxides. It must be noted that above cited field studies are based on measurements at the Northern Hemisphere USA and thus organosulfates formation pathways and sources may differ from that of Amazonia.

KMD plots are a useful visualisation technique for identification of homologous series of compounds differing only by the number of a specific base unit (e.g., a CH_2 group). Anthropogenically affected aerosol samples have longer homologous series of molecules containing CHOS subgroups (Figure 8b). One of these longer series includes a second most abundant~~intensive~~ ion at m/z 213.0075 ($\text{C}_5\text{H}_{10}\text{O}_7\text{S}$). The compound with molecular formula $\text{C}_5\text{H}_{10}\text{O}_7\text{S}$ has been previously observed in the laboratory and field studies and attributed to

isoprene derived organosulfates (Surratt et al., 2008; Gómez-González, 2008; Kristensen and Glassius, 2011; Nguyen et al., 2014; Hettiyadura et al., 2015). This molecular formula could also be associated with organosulfates (e.g., isomeric 3-sulfooxy-2-hydroxypentanoic acid and 2-sulfooxy-3-hydroxypentanoic acid) formed from the green leaf volatiles 2-*E*-pentenal, 2-*E*-hexenal, and 3-hexenal (Shalamzari et al., 2016). The KMD plot (Figure 8b) shows that OA from the anthropogenically affected samples contained an additional series of CHOS molecules with high KMD >0.33 that were not present in the sample from the less polluted period. Most of these ions are highly oxygenated (containing >10 oxygens) and are likely to be associated with molecules produced through photochemical ageing reactions (Hildebrandt et al., 2010).

It is worth noting that in ~~the~~ most of the samples IEPOX-OS was not a part of any homologous series in KMD plot (e.g., Fig 8b). This observation confirms that atmospheric oxidation reactions resulting in the incorporation of S and N functional groups do not always conserve homologous series but could also lead to a wide range of possible reaction products (Rincon et al., 2012; Kourtchev et al., 2013).

Conclusions

In this study we applied direct infusion nanoESI UHR-MS for the analysis of the organic fraction of PM_{2.5} samples collected IOP1 and IOP2 of GoAmazon2014/5 in central Amazonia which is influenced by both background and polluted air masses. Up to 2100 elemental formulae were identified in the samples, with the largest number of formulae found during IOP2. The distribution of several tracer compounds along with the comprehensive mass spectral data evaluation methods (e.g., Kendrick Mass Defect, Van Krevelen diagrams, carbon oxidation state and aromaticity equivalent) applied to the large UHRMS datasets were used to identify various sources of organic aerosol components, including natural biogenic sources, biomass burning and anthropogenic emissions. The distinguishable homologous series in the KMD diagram contained nitrogen-containing series included NACs, e.g.,

nitrocatechols, nitrophenols, nitroguaiacols and nitrosalicylic acids derived from biomass burning material. Isoprene derived IEPOX-OS was found as the most dominant ion in most of the analysed samples and strongly followed the concentration trends of the gas-phase anthropogenic tracer benzene and CO (with biomass burning as dominant tracer at the T3 site) supporting its mixed biomass burning-anthropogenic-biogenic origin. Van Krevelen, DBE and Xc distributions along with relatively low elemental O/C and H/C ratios indicated the presence of a large number of oxidised aromatic compounds in the samples. A significant number of CHO containing formulae in aerosol samples from IOP2 had higher oxidation state compared to that from IOP1 and became even more important during the days with the highest incidents of fires. Although our results suggest that the studied site is not only significantly influenced by biogenic emissions and biomass burning but also anthropogenic emissions from the neighboring urban activities, future work is needed to better understand the quantitative contributions of the various factors to the aerosol composition at the T3 site. The analysis of aerosol samples with higher sampling resolution or quantifying specific marker compounds and applying a receptor modelling techniques (Alves et al., 2015) would allow separating these sources in more detail and thus significantly improve understanding of the aerosol formation sources at the site.

Acknowledgment:

Research at the University of Cambridge was supported by the ERC grant no. 279405. The authors would like to thank Dr Jason Surratt (University of North Carolina) for providing a synthesised IEPOX-OS standard. O₃, CO, NO_y, RH and rain data were obtained from the Atmospheric Radiation Measurement (ARM) Climate Research Facility, a U.S. Department of Energy Office of Science user facility sponsored by the Office of Biological and Environmental Research. We acknowledge the support from the Central Office of the Large Scale Biosphere Atmosphere Experiment in Amazonia (LBA), the Instituto Nacional de Pesquisas da Amazonia (INPA), and the Universidade do Estado do Amazonia (UEA). The work was conducted under

535 001030/2012-4 of the Brazilian National Council for Scientific and Technological Development
536 (CNPq).

537

538

539 **References:**

540 Andreae, M. O. and Crutzen, P. J.: Atmospheric aerosols: Biogeochemical sources and role
541 in atmospheric chemistry, *Science*, 276, 1052–1058, 1997.

542 Andreae, M. O., Acevedo, O. C., Araùjo, A., Artaxo, P., Barbosa, C. G. G., Barbosa, H. M.
543 J., Brito, J., Carbone, S., Chi, X., Cintra, B. B. L., da Silva, N. F., Dias, N. L., Dias-Júnior, C.
544 Q., Ditas, F., Ditz, R., Godoi, A. F. L., Godoi, R. H. M., Heimann, M., Hoffmann, T.,
545 Kesselmeier, J., Könemann, T., Krüger, M. L., Lavric, J. V., Manzi, A. O., Lopes, A. P.,
546 Martins, D. L., Mikhailov, E. F., Moran-Zuloaga, D., Nelson, B. W., Nölscher, A. C., Santos
547 Nogueira, D., Piedade, M. T. F., Pöhlker, C., Pöschl, U., Quesada, C. A., Rizzo, L. V., Ro,
548 C.-U., Ruckteschler, N., Sá, L. D. A., de Oliveira Sá, M., Sales, C. B., dos Santos, R. M. N.,
549 Saturno, J., Schöngart, J., Sörgel, M., de Souza, C. M., de Souza, R. A. F., Su, H.,
550 Targhetta, N., Tóta, J., Trebs, I., Trumbore, S., van Eijck, A., Walter, D., Wang, Z., Weber,
551 B., Williams, J., Winderlich, J., Wittmann, F., Wolff, S., and Yáñez-Serrano, A. M.: The
552 Amazon Tall Tower Observatory (ATTO): overview of pilot measurements on ecosystem
553 ecology, meteorology, trace gases, and aerosols, *Atmos. Chem. Phys.*, 15, 10723-10776,
554 2015.

555 Alves, E. G., Jardine, K., Tota, J., Jardine, A., Yáñez-Serrano, A. M., Karl, T., Tavares, J.,
556 Nelson, B., Gu, D., Stavrakou, T., Martin, S., Manzi, A., and Guenther, A.: Seasonality of
557 isoprenoid emissions from a primary rainforest in central Amazonia, *Atmos. Chem. Phys.*
558 *Discuss.*, 15, 28867-28913, 2015.

559 Ayres, B. R., Allen, H. M., Draper, D. C., Brown, S. S., Wild, R. J., Jimenez, J. L., Day, D. A.,
560 Campuzano-Jost, P., Hu, W., de Gouw, J., Koss, A., Cohen, R. C., Duffey, K. C., Romer, P.,
561 Baumann, K., Edgerton, E., Takahama, S., Thornton, J. A., Lee, B. H., Lopez-Hilfiker, F. D.,
562 Mohr, C., Wennberg, P. O., Nguyen, T. B., Teng, A., Goldstein, A. H., Olson, K., and Fry, J.
563 L.: Organic nitrate aerosol formation via NO_3 + biogenic volatile organic compounds in the
564 southeastern United States, *Atmos. Chem. Phys.*, 15, 13377-13392, 2015.

565 Budisulistiorini, S. H., Li, X., Bairai, S. T., Renfro, J., Liu, Y., Liu, Y. J., McKinney, K. A.,
566 Martin, S. T., McNeill, V. F., Pye, H. O. T., Nenes, A., Neff, M. E., Stone, E. A., Mueller, S.,
567 Knote, C., Shaw, S. L., Zhang, Z., Gold, A., and Surratt, J. D.: Examining the effects of
568 anthropogenic emissions on isoprene-derived secondary organic aerosol formation during
569 the 2013 Southern Oxidant and Aerosol Study (SOAS) at the Look Rock, Tennessee ground
570 site, *Atmos. Chem. Phys.*, 15, 8871-8888, 2015.

571 Chen, Q., Farmer, D. K., Rizzo, L. V., Pauliquevis, T., Kuwata, M., Karl, T. G., Guenther, A.,
572 Allan, J. D., Coe, H., Andreae, M. O., Pöschl, U., Jimenez, J. L., Artaxo, P., and Martin, S.

573 T.: Submicron particle mass concentrations and sources in the Amazonian wet season
 574 (AMAZE-08), *Atmos. Chem. Phys.*, 15, 3687-3701, 2015.

575 Claeys, M., Kourtchev, I., Pashynska, V., Vas, G., Vermeylen, R., Wang, W., Cafmeyer, J.,
 576 Chi, X., Artaxo, P., Andreae, M. O., and Maenhaut, W.: Polar organic marker compounds in
 577 atmospheric aerosols during the LBA-SMOCC 2002 biomass burning experiment in
 578 ~~Rondônia~~Rondonia, Brazil: sources and source processes, time series, diel variations and
 579 size distributions, *Atmos. Chem. Phys.*, 10, 9319–9331, doi:10.5194/acp-10-9319-2010,
 580 2010.

581 Claeys, M., Vermeylen, R., Yasmeen, F., G´omez-Gonz´alez, Y., Chi, X., Maenhaut, W.,
 582 Meszaros, T., and Salma, I.: Chemical characterisation of humic-like substances from urban,
 583 rural and tropical biomass burning environments using liquid chromatography with UV/vis
 584 photodiode array detection and electrospray ionisation mass spectrometry, *Environ. Chem.*,
 585 9, 273–284, doi:10.1071/EN11163, 2012.

586 Davies, T., Cullen, M. J. P., Malcolm, A. J., Mawson, M. H., Staniforth, A., White, A. A., and
 587 Wood, N.: A new dynamical core for the Met Office’s global and regional modelling of the
 588 atmosphere, *Q. J. Roy. Meteorol. Soc.*, 131, 1759–1782, 2005.

589 Day, D. A., Liu, S., Russell, L. M. and Ziemann, P. J.: Organonitrate group concentrations in
 590 submicron particles with high nitrate and organic fractions in coastal southern California,
 591 *Atmos. Environ.*, 44, 1970-1979, 2010.

592 de Gouw, J. A., Middlebrook, A. M., Warneke, C., Goldan, P. D., Kuster, W. C., Roberts, J.
 593 M., Fehsenfeld, F. C., Worsnop, D. R., Canagaratna, M. R., Pszenny, A. A. P., Keene, W.
 594 C., Marchewka, M., Bertman, S. B., and Bates, T. S.: Budget of organic carbon in a polluted
 595 atmosphere: Results from the New England Air Quality Study in 2002, *J. Geophys. Res.-*
 596 *Atmos.*, 110, D16305, doi:10.1029/2004jd005623, 2005.

597 Dzepina, K., Mazzoleni, C., Fialho, P., China, S., Zhang, B., Owen, R. C., Helmig, D.,
 598 Hueber, J., Kumar, S., Perlinger, J. A., Kramer, L. J., Dziobak, M. P., Ampadu, M. T., Olsen,
 599 S., Wuebbles, D. J., and Mazzoleni, L. R.: Molecular characterization of free tropospheric
 600 aerosol collected at the Pico Mountain Observatory: a case study with a long-range
 601 transported biomass burning plume, *Atmos. Chem. Phys.*, 15, 5047-5068, 2015.

602 Friedli, H. R., E. Atlas, V. R. Stroud, L. Giovanni, T. Campos, and L. F. Radke: Volatile
 603 organic trace gases emitted from North American wildfires, *Global Biogeochem. Cycles*, 15,
 604 435–452, 2001.

605 Fry, J. L., Draper, D. C., Barsanti, K. C., Smith, J. N., Ortega, J., Winkler, P. M., Lawler, M.
 606 J., Brown, S. S., Edwards, P. M., Cohen, R. C., and Lee, L.: Secondary organic aerosol
 607 formation and organic nitrate yield from NO₃ oxidation of biogenic hydrocarbons, *Environ.*
 608 *Sci. Technol.*, 48, 11944–11953, 2014.

609 Galanter, M., Levy II, H., and Carmichael, G. R.: Impacts of biomass burning on tropospheric
 610 CO, NO_x, and O₃, *J. Geophys. Res.*, 105, 6633–6653, 2000.

611 Graus, M., Müller, M. and Hansel, A.: High Resolution PTR-TOF: Quantification and Formula
 612 Confirmation of VOC in Real Time, *J. Am. Soc. Mass Spectrom.*, 21, 1037-1044, 2010.

613 Greenberg, J., Guenther, A., Petron, G., Wiedinmyer, C., Vega, O., Gatti, L. V., Tota, J., and
 614 Fisch, G.: Biogenic VOC emissions from forested Amazonian landscapes, *Global Change*
 615 *Biol.*, 10(5), 651–662, 2004.

616 Gómez-González, Y., Surratt, J. D., Cuyckens, F., Szmigielski, R., Vermeylen, R., Jaoui, M.,
 617 Lewandowski, M., Offenberg, J. H., Kleindienst, T. E., Edney, E. O., Blockhuys, F., Van
 618 Alsenoy, C., Maenhaut, W., and Claeys, M.: Characterization of organosulfates from the
 619 photooxidation of isoprene and unsaturated fatty acids in ambient aerosol using liquid
 620 chromatography/(–) electrospray ionization mass spectrometry, *J. Mass Spectrom.*, 43, 371–
 621 382, 2008.

622 Goldstein, A. H. and Galbally, I. E.: Known and unexplored organic carbon constituents in
 623 the Earth's atmosphere, *Environ. Sci. Technol.*, 41, 1514–1521, 2007.

624 Goldstein, A. H., Koven, C. D., Heald, C. L., and Fung, I. Y.: Biogenic carbon and
 625 anthropogenic pollutants combine to form a cooling haze over the southeastern United
 626 States, *P. Natl. Acad. Sci. USA*, 106, 8835–8840, 2009.

627 Hallquist, M., Wenger, J. C., Baltensperger, U., Rudich, Y., Simpson, D., Claeys, M.,
 628 Dommen, J., Donahue, N. M., George, C., Goldstein, A. H., Hamilton, J. F., Herrmann, H.,
 629 Hoffmann, T., Iinuma, Y., Jang, M., Jenkin, M. E., Jimenez, J. L., Kiendler-Scharr, A.,
 630 Maenhaut, W., McFiggans, G., Mentel, Th. F., Monod, A., Prevot, A. S. H., Seinfeld, J. H.,
 631 Surratt, J. D., Szmigielski, R., and Wildt, J.: The formation, properties and impact of
 632 secondary organic aerosol: current and emerging issues, *Atmos. Chem. Phys.*, 9, 5155–
 633 5235, 2009.

634 Haywood, J. and Boucher, O.: Estimates of the direct and indirect radiative forcing due to
 635 tropospheric aerosols: A review, *Rev. Geophys.*, 38, 513–543, 2000.

636 Hildebrandt, L., Engelhart, G. J., Mohr, C., Kostenidou, E., Lanz, V. A., Bougiatioti, A.,
 637 DeCarlo, P. F., Prevot, A. S. H., Baltensperger, U., Mihalopoulos, N., Donahue, N. M., and
 638 Pandis, S. N.: Aged organic aerosol in the Eastern Mediterranean: the Finokalia Aerosol
 639 Measurement Experiment – 2008, *Atmos. Chem. Phys.*, 10, 4167–4186, 2010.

640 Hettiyadura, A. P. S., Stone, E. A., Kundu, S., Baker, Z., Geddes, E., Richards, K., and
 641 Humphry, T.: Determination of atmospheric organosulfates using HILIC chromatography with
 642 MS detection, *Atmos. Meas. Tech.*, 8, 2347–2358, 2015.

643 Hoyle, C. R., Boy, M., Donahue, N. M., Fry, J. L., Glasius, M., Guenther, A., Hallar, A. G.,
 644 Huff Hartz, K., Petters, M. D., Petaja, T., Rosenoern, T., and Sullivan, A. P.: A review of the
 645 anthropogenic influence on biogenic secondary organic aerosol, *Atmos. Chem. Phys.*, 11,
 646 321–343, 2011.

647 Iinuma, Y., Borge, O., Grafe, R., and Herrmann, H.: Methyl-Nitrocatechols: atmospheric
 648 tracer compounds for biomass burning secondary organic aerosols, *Environ. Sci. Technol.*,
 649 44, 8453–8459, 2010.

650 Jacobson, M. Z.: Isolating nitrated and aromatic aerosols and nitrated aromatic gases as
 651 sources of ultraviolet light absorption, *J. Geophys. Res. Atmospheres*, 104 (D3), 3527–3542,
 652 1999.

653 Jacobs, M. I., Burke, W.J., and Elrod, M.K.: Kinetics of the reactions of isoprene-derived
 654 hydroxynitrates: Gas phase epoxide formation and solution phase hydrolysis, *Atmos. Chem.*
 655 *Phys.*, 14, 8933–8946, 2014.

656 Kahnt, A., Behrouzi, S., Vermeylen, R., Safi Shalamzari, M., Vercauteren, J., Roekens, E.,
 657 Claeys, M., and Maenhaut, W.: One year study of nitro-organic compounds and their relation
 658 to wood burning in PM10 aerosol from a rural site in Belgium, *Atmos. Environ.*, 81, 561–568,
 659 2013.

660 Kendrick E.: A Mass Scale Based on $\text{CH}_2 = 14.0000$ for High Resolution Mass Spectrometry
 661 of Organic Compounds, *Anal. Chem.*, 35 (13), 2146–2154, 1963.

662 Keller, M., Bustamante, M., Gash, J., and Dias, P.: Amazonia and Global Change, Vol. 186,
 663 American Geophysical Union, Wiley, Washington, D.C., 2009.

664 Kitanovski, Z., Grgić, I., Vermeylen, R., Claeys, M., and Maenhaut, W.: Liquid
 665 chromatography tandem mass spectrometry method for characterization of monoaromatic
 666 nitro-compounds in atmospheric particulate matter, *J. Chromatogr. A*, 1268, 35–43, 2012a.

667 Kitanovski, Z., Grgic, I., Yasmeen, F., Claeys, M., and Cusak, A.: Development of a liquid
 668 chromatographic method based on ultraviolet-visible and electrospray ionization mass
 669 spectrometric detection for the identification of nitrocatechols and related tracers in biomass
 670 burning atmospheric organic aerosol, *Rapid Commun. Mass Sp.*, 26, 793–804, 2012b.

671 Kourtchev, I., Hellebust, S., Bell, J. M., O'Connor, I. P., Healy, R. M., Allanic, A., Healy, D.,
 672 Wenger, J. C., and Sodeau, J. R.: The use of polar organic compounds to estimate the
 673 contribution of domestic solid fuel combustion and biogenic sources to ambient levels of
 674 organic carbon and PM2.5 in Cork Harbour, Ireland, *Sci.Total Environ.*, 409, 2143–2155,
 675 2011.

676 Kourtchev, I., Fuller, S., Aalto, J., Ruuskanen, T. M., McLeod, M. W., Maenhaut, W., Jones,
 677 R., Kulmala, M., and Kalberer, M.: Molecular composition of boreal forest aerosol from
 678 Hyytiälä, Finland, using ultrahigh resolution mass spectrometry, *Environ. Sci. Technol.*, 47,
 679 4069–4079, 2013.

680 Kourtchev, I., O'Connor, I. P., Giorio, C., Fuller, S., Kristensen, K., Maenhaut, W., Wenger,
 681 J. C., Sodeau, J. R., Glasius, M., and Kalberer, M.: Effects of anthropogenic emissions on
 682 the molecular composition of urban organic aerosols: an ultrahigh resolution mass
 683 spectrometry study, *Atmos. Environ.*, 89, 525-532, 2014.

684 Kourtchev, I., Doussin, J.-F., Giorio, C., Mahon, B., Wilson, E. M., Maurin, N., Pangu, E.,
 685 Venables, D. S., Wenger, J. C., and Kalberer, M.: Molecular composition of fresh and aged
 686 secondary organic aerosol from a mixture of biogenic volatile compounds: a high-resolution
 687 mass spectrometry study, *Atmos. Chem. Phys.*, 15, 5683-5695, 2015.

688 Kristensen, K. and Glasius, M.: Organosulfates and oxidation products from biogenic
 689 hydrocarbons in fine aerosols from a forest in North West Europe during spring, *Atmos.*
 690 *Environ.*, 45, 4546–4556, 2011.

691 Kroll, J. H., Donahue, N. M., Jimenez, J. L., Kessler, S. H., Canagaratna, M. R., Wilson, K.
 692 R., Altieri, K. E., Mazzoleni, L. R., Wozniak, A. S., Bluhm, H., Mysak, E. R., Smith, J. D.,

693 Kolb, C. E., and Worsnop, D. R.: Carbon oxidation state as a metric for describing the
694 chemistry of atmospheric organic aerosol, *Nat. Chem. Biol.*, 3, 133–139, 2011.

695 Kleinman, L., Kuang, C., Sedlacek, A., Senum, G., Springston, S., Wang, J., Zhang, Q.,
696 Jayne, J., Fast, J., Hubbe, J., Shilling, J., and Zaveri, R.: What do correlations tell us about
697 anthropogenic–biogenic interactions and SOA formation in the Sacramento Plume during
698 CARES?, *Atmos. Chem. Phys. Discuss.*, 15, 25381–25431, 2015.

699 Kuang, B.Y., Lin, P., Hub, M., and Yu, J.Z.: Aerosol size distribution characteristics of
700 organosulfates in the Pearl River Delta region, China, *Atmos. Environ.*, 130, 23–35, 2016.

701 Laskin, A., Laskin, J., and Nizkorodov, S. A.: Chemistry of Atmospheric Brown Carbon,
702 *Chem. Rev.*, 115, 4335–4382, 2015.

703 Liao, J., Froyd, K. D., Murphy, D. M., Keutsch, F. N., Yu, G., Wennberg, P. O., St. Clair, J.
704 M., Crounse, J. D., Wisthaler, A., Mikoviny, T., Jimenez, J. L., Campuzano-Jost, P., Day, D.
705 A., Hu, W., Ryerson, T. B., Pollack, I. B., Peischl, J., Anderson, B.E., Ziemba, L. D., Blake,
706 D. R., Meinardi, S., and Diskin, G.: Airborne measurements of organosulfates over the
707 continental U. S., *J. Geophys. Res.*, 120, 2990–3005, doi: 10.1002/2014JD022378, 2015.

708 Lin, Y. H., Zhang, Z. F., Docherty, K. S., Zhang, H. F., Budisulistiorini, S. H., Rubitschun, C.
709 L., Shaw, S. L., Knipping, E. M., Edgerton, E. S., Kleindienst, T. E., Gold, A., and Surratt, J.
710 D.: Isoprene Epoxydiols as Precursors to Secondary Organic Aerosol Formation: Acid-
711 Catalyzed Reactive Uptake Studies with Authentic Compounds, *Environ. Sci. Technol.*, 46,
712 250–258, 2012.

713 Lin, Y.-H., Knipping, E. M., Edgerton, E. S., Shaw, S. L., and Surratt, J. D.: Investigating the
714 influences of SO₂ and NH₃ levels on isoprene-derived secondary organic aerosol formation
715 using conditional sampling approaches, *Atmos. Chem. Phys.*, 13, 8457–8470, 2013.

716 Lu, J. W., Flores, J. M., Lavi, A., Abo-Riziq, A., and Rudich, Y.: Changes in the optical
717 properties of benzo[a]pyrene-coated aerosols upon heterogeneous reactions with NO₂ and
718 NO₃, *Phys. Chem. Chem. Phys.*, 13, 6484–6492, 2011.

719 Malloy, Q. G. J., Li Qi, Warren, B., Cocker III, D. R., Erupe, M. E., and Silva, P. J.:
720 Secondary organic aerosol formation from primary aliphatic amines with NO₃ radical, *Atmos.*
721 *Chem. Phys.*, 9, 2051–2060, 2009.

722 Martin, S. T., Artaxo, P., Machado, L. A. T., Manzi, A. O., Souza, R. A. F., Schumacher, C.,
723 Wang, J., Andreae, M. O., Barbosa, H. M. J., Fan, J., Fisch, G., Goldstein, A. H., Guenther,
724 A., Jimenez, J. L., Pöschl, U., Silva Dias, M. A., Smith, J. N., and Wendisch, M.: Introduction:
725 Observations and Modeling of the Green Ocean Amazon (GoAmazon2014/5), *Atmos.*
726 *Chem. Phys.*, 16, 4785–4797, 2016.

727 Martin, S. T., Andreae, M. O., Artaxo, P., Baumgardner, D., Chen, Q., Goldstein, A. H.,
728 Guenther, A., Heald, C. L., Mayol-Bracero, O. L., McMurry, P. H., Pauliquevis, T., Pöschl, U.,
729 Prather, K. A., Roberts, G. C., Saleska, S. R., Silva Dias, M. A., Spracklen, D. V., Swietlicki,
730 E., and Trebs, I.: Sources and properties of Amazonian aerosol particles, *Rev. Geophys.*, 48,
731 RG2002, doi:10.1029/2008RG000280, 2010.

732 Maryon, R.H., Smith, F.B., Conway, B.J., Goddard, D.M.: The U.K. nuclear accident model,
733 Prog. Nucl. Energy 26, 85-104, 1991.

734 Mazzoleni, L. R., Ehrmann, B. M., Shen, X., Marshall, A. G., and Collett Jr., J. L.: Water-
735 soluble atmospheric organic matter in fog: exact masses and chemical formula identification
736 by ultrahighresolution Fourier transform ion cyclotron resonance mass spectrometry,
737 Environ. Sci. Technol., 44, 3690–3697, 2010.

738 Mazzoleni, L. R., Saranjampour, P., Dalbec, M. M., Samburova, V., Hallar, A. G., Zielinska,
739 B., Lowenthal, D., and Kohl, S.: Identification of water-soluble organic carbon in nonurban
740 aerosols using ultrahigh-resolution FT-ICR mass spectrometry: organic anions, Environ.
741 Chem., 9, 285–297, 2012.

742 Müller, M., Mikoviny, T., Jud, W., D'Anna, B., and Wisthaler, A.: A New Software Tool for the
743 Analysis of High Resolution PTR-TOF Mass Spectra, Chemometr. Intell. Lab., 127, 158-165,
744 2013.

745 Nguyen, Q. T., Christensen, M. K., Cozzi, F., Zare, A., Hansen, A. M. K., Kristensen, K.,
746 Tulinius, T. E., Madsen, H. H., Christensen, J. H., Brandt, J., Massling, A., Nøjgaard, J. K.,
747 and Glasius, M.: Understanding the anthropogenic influence on formation of biogenic
748 secondary organic aerosols in Denmark via analysis of organosulfates and related oxidation
749 products, Atmos. Chem. Phys., 14, 8961-8981, 2014.

750 Nizkorodov, S. A., Laskin, J., and Laskin, A.: Molecular chemistry of organic aerosols
751 through the application of high resolution mass spectrometry, Phys. Chem. Chem. Phys., 13,
752 3612–3629, 2011.

753 Nozière, B., Kalberer, M., Claeys, M., Allan, J., D'Anna, B., Decesari, S., Finessi, E.,
754 Glasius, M., Grgic, I., Hamilton, J. F., Hoffmann, T., Iinuma, Y., Jaoui, M., Kahnt, A., Kampf,
755 C. J., Kourtchev, I., Maenhaut, W., Marsden, N., Saarikoski, S., Schnelle-Kreis, J., Surratt,
756 J., Szidat, S., Szmigielski, R., and Wisthaler, S.: The molecular identification of organic
757 compounds in the atmosphere: state of the art and challenges, Chem. Rev., 115, 3919–
758 3983, 2015.

759 Oss, M., Kruve, A., Herodes, K., and Leito, I.: Electrospray ionization efficiency scale of
760 organic compounds, Anal. Chem., 82, 2865–2872, 2010.

761 Pashynska, V., Vermeylen, R., Vas, G., Maenhaut, W., and Claeys, M.: Development of a
762 gas chromatographic/ion trap mass spectrometric method for the determination of
763 levoglucosan and saccharidic compounds in atmospheric aerosols. Application to urban
764 aerosols. J. Mass Spec., 37, 1249–1257, 2002.

765 Pöschl, U., Martin, S. T., Sinha, B., Chen, Q., Gunthe, S. S., Huffman, J. A., Borrmann, S.,
766 Farmer, D. K., Garland, R. M., Helas, G., Jimenez, J. L., King, S. M., Manzi, A., Mikhailov,
767 E., Pauliquevis, T., Petters, M. D., Prenni, A. J., Roldin, P., Rose, D., Schneider, J., Su, H.,
768 Zorn, S. R., Artaxo, P., and Andreae, M. O.: Rainforest aerosols as biogenic nuclei of clouds
769 and precipitation in the Amazon, Science, 429, 1513–1516, 2010.

770 Pye, H. O. T., Pinder, R. W., Piletic, I. R., Xie, Y., Capps, S. L., Lin, Y.-H., Surratt, J. D.,
771 Zhang, Z., Gold, A., Luecken, D. J., Hutzell, W. T., Jaoui, M., Offenberg, J. H., Kleindienst,
772 T. E., Lewandowski, M., and Edney, E. O.: Epoxide pathways improve model predictions of

773 isoprene markers and reveal key role of acidity in aerosol formation, *Environ. Sci. Technol.*,
774 47, 11056–11064, 2013.

775 Rasmussen, R.A. and Khalil, M.A.K.: Isoprene over the Amazon Basin. *J. Geophys. Res.*,
776 93: 1417-1427. doi: 10.1029/JD093iD02p01417JD093iD02p01417, 1988.

777 Reemtsma, T.: Determination of molecular formulas of natural organic matter molecules by
778 (ultra-) high-resolution mass spectrometry status and needs, *J. Chromatogr. A*, 1216, 3687-
779 3701, 2009.

780 Riva, M., Tomaz, S., Cui, T., Lin, Y.-H., Perraudin, E., Gold, A., Stone, E. A., Villenave, E.,
781 and Surratt, J. D.: Evidence for an unrecognized secondary anthropogenic source of
782 organosulfates and sulfonates: gas-phase oxidation of polycyclic aromatic hydrocarbons in
783 the presence of sulfate aerosol, *Environ. Sci. Technol.*, 49, 6654-6664, 2015.

784 Riva, M., Da Silva Barbosa, T., Lin, Y.-H., Stone, E. A., Gold, A., and Surratt, J. D.:
785 Characterization of Organosulfates in Secondary Organic Aerosol Derived from the
786 Photooxidation of Long-Chain Alkanes, *Atmos. Chem. Phys. Discuss.*, doi:10.5194/acp-
787 2016-20, 2016.

788 Ryall, D. B. and Maryon, R. H.: Validation of the UK Met Office's NAME model against the
789 ETEX dataset, *Atmos. Environ.*, 32, 4265–4276, 1998.

790 Roberts, J. M.: The atmospheric chemistry of organic nitrates. *Atmos. Environ.*, 24,243-287,
791 1990.

792 Rincón, A. G., Calvo, A. I., Dietzel, M., and Kalberer, M.: Seasonal differences of urban
793 organic aerosol composition: an ultra-high resolution mass spectrometry study. *Environ.*
794 *Chem.*, 9, 298-319, 2012.

795 Schmitt-Kopplin, P., Gelencsér, A., Dabek-Zlotorzynska, E., Kiss, G., Hertkorn, N., Harir, M.,
796 Hong, Y., and Gebefügi, I.: Analysis of the unresolved organic fraction in atmospheric
797 aerosols with ultrahigh-resolution mass spectrometry and nuclear magnetic resonance
798 spectroscopy: Organosulfates as photochemical smog constituents, *Anal. Chem.*, 82, 8017–
799 8026, 2010.

800 Seco, R., Peñuelas, J., Filella, I., Llusia, J., Schallhart, S., Metzger, A., Müller, M., and
801 Hansel, A.: Volatile Organic Compounds in the Western Mediterranean Basin: urban and
802 rural winter measurements during the DAURE campaign, *Atmos. Chem. Phys.*, 13: 4291-
803 4306, 2013.

804 Shalamzari, M. S., Vermeylen, R., Blockhuys, F., Kleindienst, T. E., Lewandowski, M.,
805 Szmigielski, R., Rudzinski, K. J., Spólnik, G., Danikiewicz, W., Maenhaut, W., and Claeys,
806 M.: Characterization of polar organosulfates in secondary organic aerosol from the
807 unsaturated aldehydes 2-*E*-pentenal, 2-*E*-hexenal, and 3-*Z*-hexenal, *Atmos. Chem. Phys.*,
808 16, 7135-7148, 2016.

809 Simoneit, B. R. T., Schauer, J. J., Nolte, C. G., Oros, D. R., Elias, V. O., Fraser, M. P.,
810 Rogge, W. F. and Cass, G. R.: Levoglucosan, a tracer for cellulose in biomass burning and
811 atmospheric particles. *Atmos. Environ.*, 33, 173–182, 1999.

812 Surratt, J. D., Lewandowski, M., Offenberg, J. H., Jaoui, M., Kleindienst, T. E., Edney, E. O.,
813 and Seinfeld, J. H.: Effect of acidity on secondary organic aerosol formation from isoprene,
814 *Environ. Sci. Technol.*, 41, 5363–5369, 2007.

815 Surratt, J. D., Gomez-Gonzalez, Y., Chan, A. W. H., Vermeylen, R., Shahgholi, M.,
816 Kleindienst, T. E., Edney, E. O., Offenberg, J. H., Lewandowski, M., Jaoui, M., Maenhaut,
817 W., Claeys, M., Flagan, R. C., and Seinfeld, J. H.: Organosulfate formation in biogenic
818 secondary organic aerosol, *J. Phys. Chem. A*, 112, 8345–8378, 2008.

819 Surratt, J. D., Chan, A. W. H., Eddingsaas, N. C., Chan, M. N., Loza, C. L., Kwan, A. J.,
820 Hersey, S. P., Flagan, R. C., Wennberg, P. O., and Seinfeld, J. H.: Reactive intermediates
821 revealed in secondary organic aerosol formation from isoprene, *P. Natl. Acad. Sci. USA*,
822 107, 6640–6645, 2010.

823 Song, C., Gyawali, M., Zaveri, R. A., Shilling, J. E., and Arnott, W. P.: Light absorption by
824 secondary organic aerosol from α -pinene: Effects of oxidants, seed aerosol acidity, and
825 relative humidity, *J. Geophys. Res.*, 118 (20), 11741–11749, doi: 10.1002/jgrd.50767, 2013.

826 Szmigielski, R., Surratt, J. D., Gomez-Gonzalez, Y., Van der Veken, P., Kourtchev, I.,
827 Vermeylen, R., Blockhuys, F., Jaoui, M., Kleindienst, T. E., Lewandowski, M., Offenberg, J.
828 H., Edney, E. O., Seinfeld, J. H., Maenhaut, W., and Claeys, M.: 3-methyl-1,2,3-
829 butanetricarboxylic acid: An atmospheric tracer for terpene secondary organic aerosol,
830 *Geophys. Res. Lett.*, 34, L24811, doi:10.1029/2007GL031338, 2007.

831 Tao, S., Lu, X., Levac, N., Bateman, A. P., Nguyen, T. B., Bones, D. L., Nizkorodov, S. A.,
832 Laskin, J., Laskin, A., and Yang, X.: Molecular characterization of organosulfates in organic
833 aerosols from Shanghai and Los Angeles urban areas by nanospray-desorption electrospray
834 ionization high-resolution mass spectrometry, *Environ. Sci. Technol.*, 48, 10993–11001,
835 2014.

836 Tong, H., Kourtchev, I., Pant, P., Keyte, I., O'Connor, I., Wenger, J., Pope, F.D., Harrison,
837 R.M., and Kalberer, M.: FDATMOS16 Molecular Composition of Organic Aerosols at Urban
838 Background and Road Tunnel sites using Ultra-high Resolution Mass Spectrometry, *Faraday*
839 *Discuss.*, DOI: 10.1039/C5FD00206K, 2016.

840 Wang, X.K., Rossignol, S., Ma, Y., Yao, L., Wang, M.Y., Chen, J.M., George, C., and Wang,
841 L.: Identification of particulate organosulfates in three megacities at the middle and lower
842 reaches of the Yangtze River, *Atmos. Chem. Phys. Discuss.*, 15, 21414–21448, 2015.

843 Wozniak, A. S., Bauer, J. E., Sleighter, R. L., Dickhut, R. M., and Hatcher, P. G.: Technical
844 Note: Molecular characterization of aerosol-derived water soluble organic carbon using
845 ultrahigh resolution electrospray ionization Fourier transform ion cyclotron resonance mass
846 spectrometry, *Atmos. Chem. Phys.*, 8, 5099–5111, 2008.

847 Yassine, M. M., Harir, M., Dabek-Zlotorzynska, E., and Schmitt-Kopplin, P.: Structural
848 characterization of organic aerosol using Fourier transform ion cyclotron resonance mass
849 spectrometry: aromaticity equivalent approach. *Rapid Commun. Mass Sp.*, 28, 2445–2454,
850 2014.

851 Zahardis, J., Geddes, S., and Petrucci, G. A.: The ozonolysis of primary aliphatic amines in
852 fine particles, *Atmos. Chem. Phys.*, 8, 1181–1194, 2008.

Zhao, Y., Hallar, A. G., and Mazzoleni, L. R.: Atmospheric organic matter in clouds: exact masses and molecular formula identification using ultrahigh-resolution FT-ICR mass spectrometry, *Atmos. Chem. Phys.*, 13, 12343-12362, 2013.

Figures:

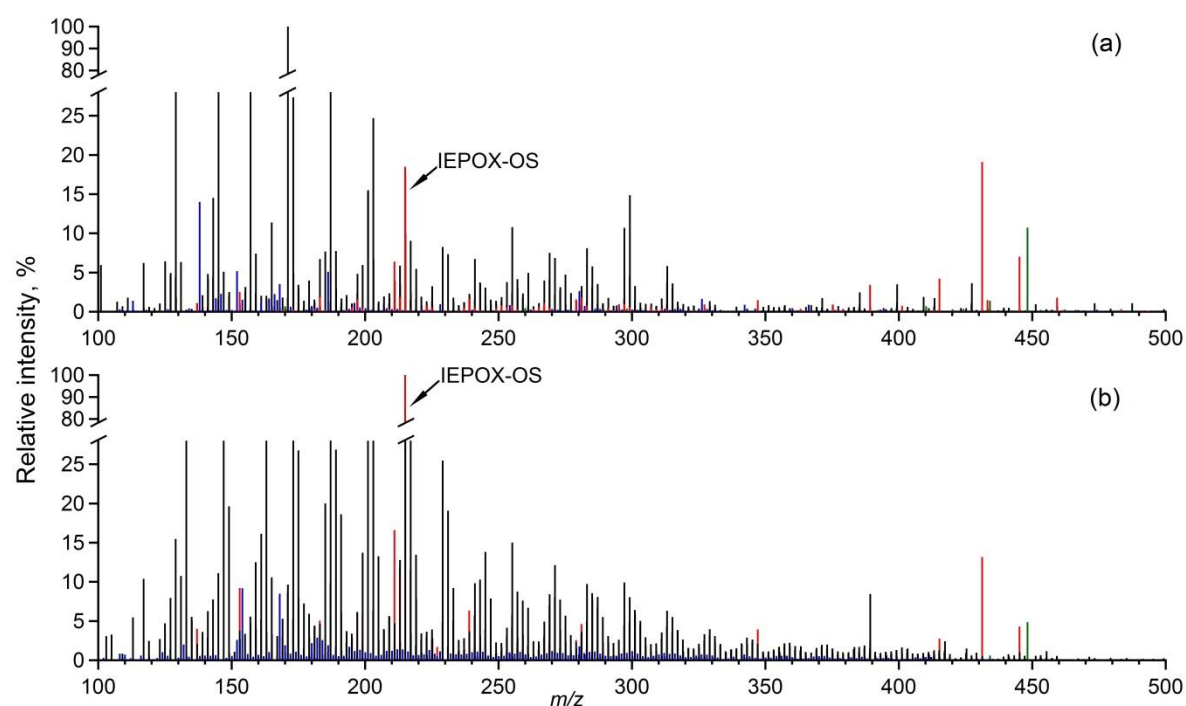
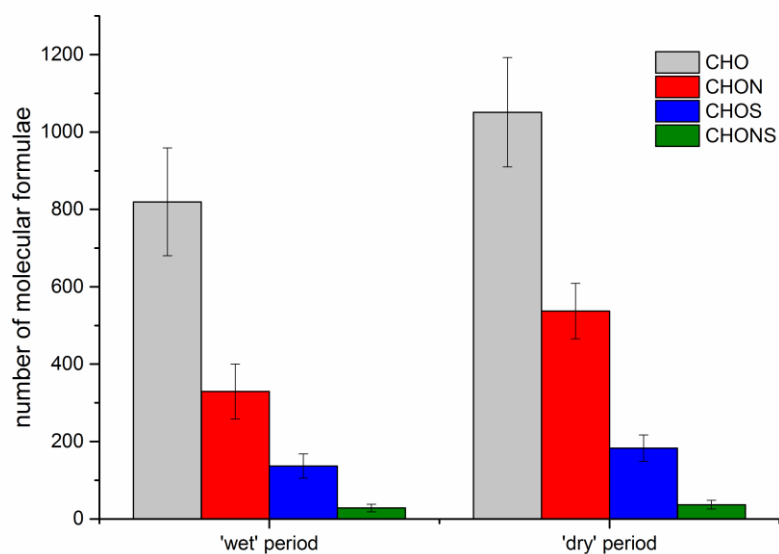
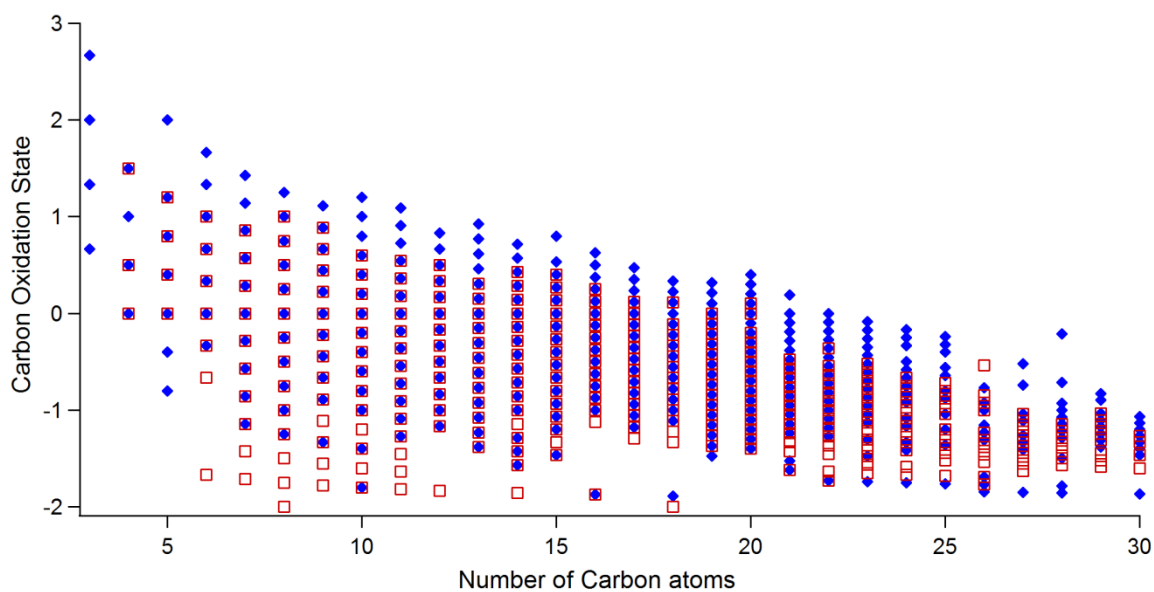


Figure 1. (-)-nanoESI-UHRMS of the representative PM_{2.5} samples during (a) IOP1 (b) IOP2. The line colours in the mass spectra correspond to the CHO (black), blue (CHON), CHOS (red) and CHONS (green) formulae assignments. The relative intensity axis was split to make a large number of ions with low intensities visible.



866

867 Figure 2. Average number of molecular formulae during IOP1 and IOP2. Standard deviation
868 bars show variations between samples within individual season.



869

870 Figure 3. Carbon oxidation state plot for CHO containing formulae in organic aerosol from
871 IOP1 (red squares) and IOP2 (blue diamonds).

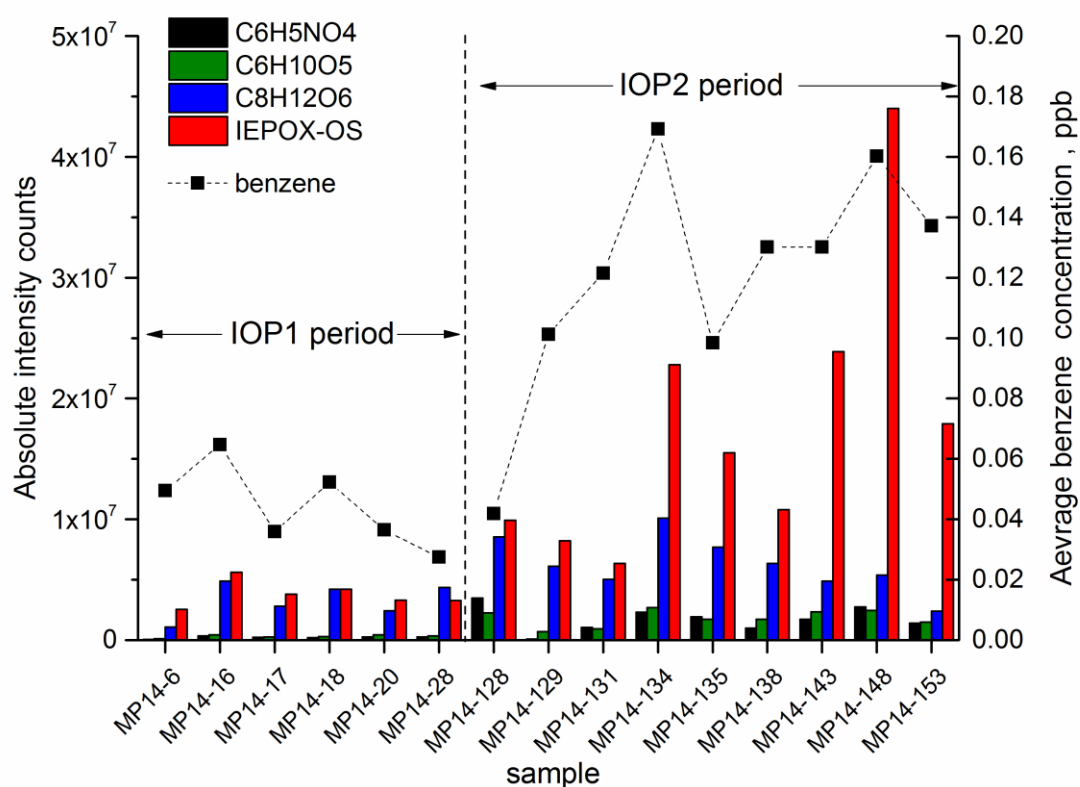


Figure 4. Ion intensity distributions (left axis) of selected tentatively identified markers in individual samples using UHRMS analysis and averaged benzene concentration (right axis) from PTR-TOF-MS analysis. Benzene concentration was averaged for the aerosol filter sampling intervals. The UHRMS data was corrected for organic carbon load in each individual filter sample (see method section).

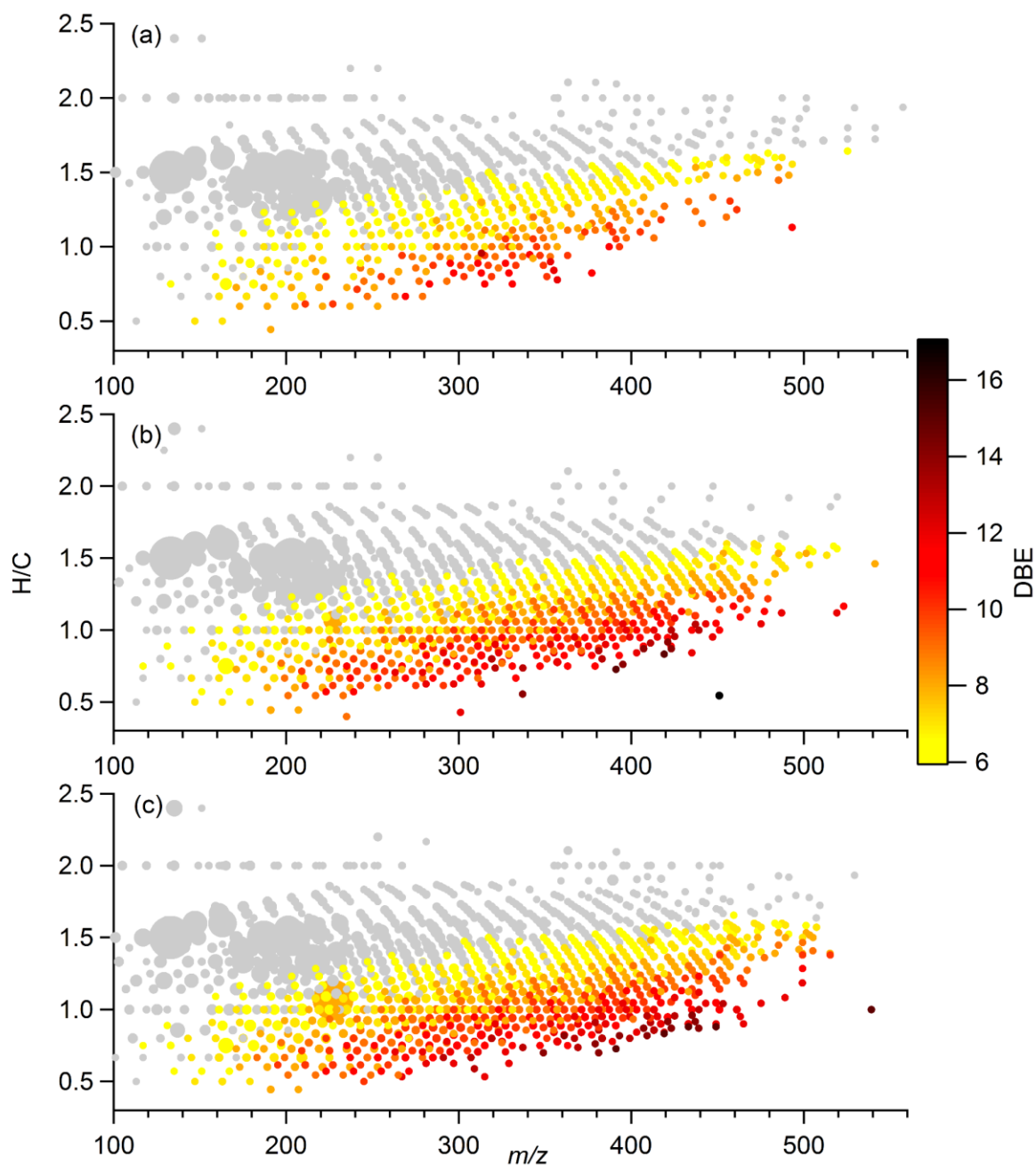


Figure 5. H/C vs m/z plot for CHO containing formulae in the samples from the periods with (a) low (b) moderately high and (c) very high incidents of fires. The marker areas reflect relative ion abundance in the sample. The colour code shows double bond equivalent (DBE) in the individual molecular formula. Molecular formulae with $\text{DBE} < 6$ are shown as grey markers. The largest grey circles correspond to the ions at m/z 133.01425 (with neutral molecular formula $\text{C}_4\text{H}_6\text{O}_5$), m/z 187.0612 ($\text{C}_8\text{H}_{12}\text{O}_5$), m/z 201.07685 ($\text{C}_9\text{H}_{14}\text{O}_5$), m/z 203.05611 ($\text{C}_8\text{H}_{12}\text{O}_6$), and m/z 215.05611 ($\text{C}_9\text{H}_{12}\text{O}_6$).

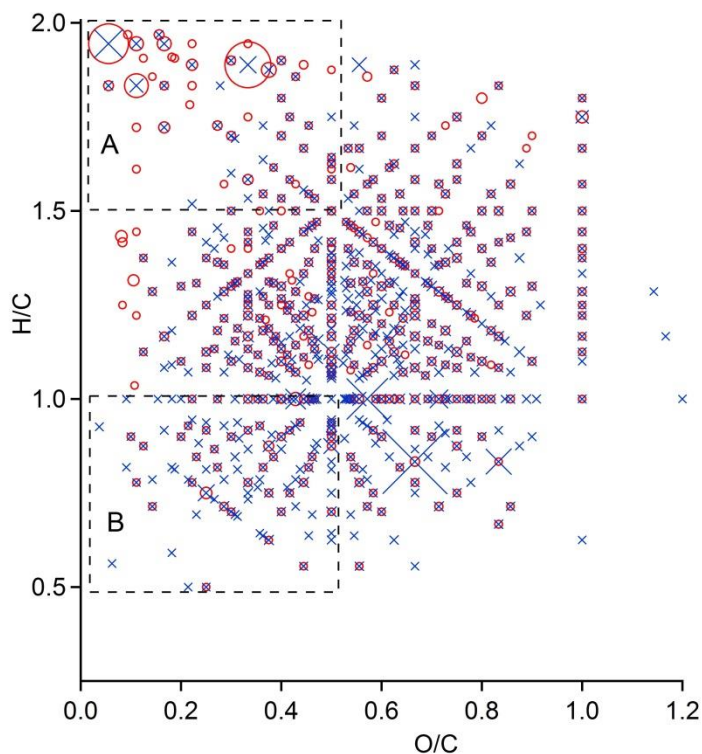


Figure 6. Overlaid Van Krevelen diagrams for CHON containing formulae in the samples from the periods with low (red markers) and very high incidents of fires. The marker areas reflect relative ion abundance in the sample. Areas 'A' and 'B' indicate differences in the number of ions tentatively attributed to aliphatic and aromatic species, respectively.

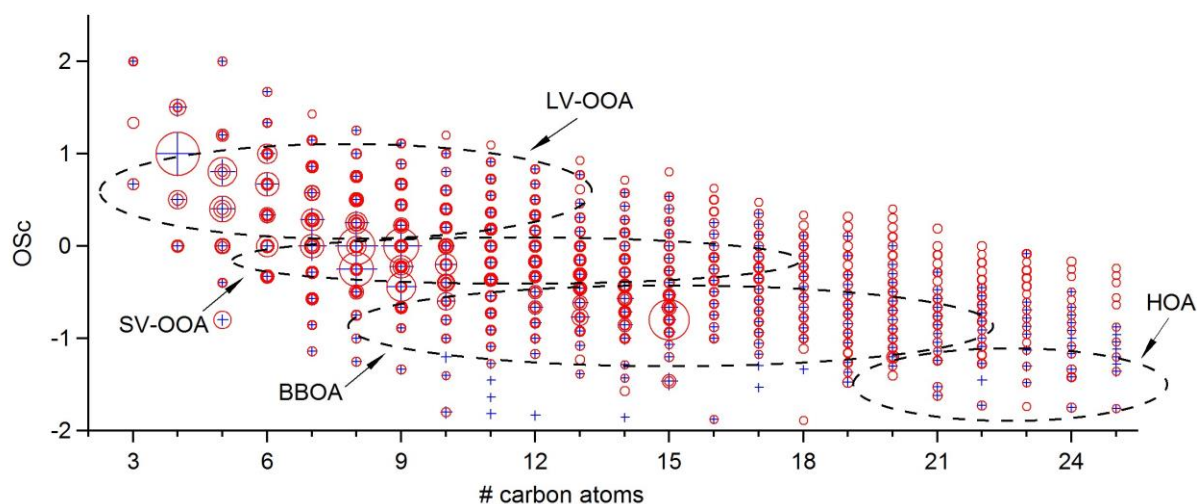
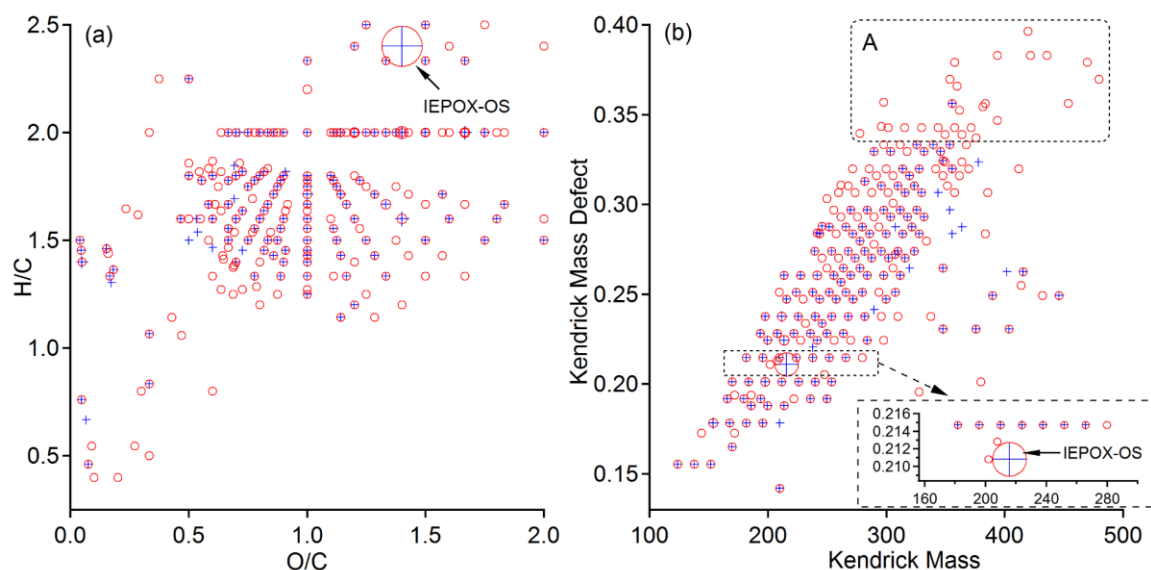


Figure 7. Overlaid carbon oxidation state (OSc) plots for CHO subgroups in the samples from the periods with low (blue markers) and very high incidents of fires. The marker areas reflect relative ion abundance in the sample. The area marked as SV-OOA, LV-OOA, BBOA and HOA correspond to the molecules associated with semivolatile and low-volatility oxidised organic aerosol, biomass burning organic aerosol and hydrocarbon-like organic aerosol as outlined by Kroll et al. (2011).

903



904

905 Figure 8. Overlaid Van Krevelen diagram (a) and Kendrick Mass Defect plot (b) for CHOS
 906 containing formulae in the samples from the periods with low (blue markers) and very high
 907 incidents of fires (red markers). The marker areas reflect relative ion abundance in the
 908 sample. Red markers correspond to the ions from the period with the lowest incidents of
 909 fires. Note that IEPOX-OS is not a part of any homologous series in the sample with very low
 910 incident of fires and only one additional homologue in the sample that experienced very high
 911 incident of fires (see enlarged area of the Fig 8a). Area 'A' in Kendrick Mass Defect (KMD)
 912 plot shows formulae with KMD>0.33 that are mainly present in the sample with high incident
 913 of fires.

914

915